11

Study of a COVID-19 mathematical model

Tariq Hussain, Eiman, Hayat Ullah, Khalid Mahmood, Muhammad Arfan, Rozi Gul, and Kamal Shah

DEPARTMENT OF MATHEMATICS, UNIVERSITY OF MALAKAND, KHYBER PAKHTUNKHWA, PAKISTAN

1 Introduction

The COVID-19 virus first occurred in Wuhan, China in December 2019. COVID-19 has been named novel because it is a completely new variant (genetically variant, chain) of virus and due to emerging in the year 2019, it was given the numerical suffix 19. The said virus survives on surfaces of human body variably ranging from few hours to several days and causes complications for the respiratory system of the human population across the whole world. Coronavirus is considered to be the most challenging virus of the community of flu viruses. As the transmission of coronavirus occurs, we must be aware of the fact that the future will involve a war between health and disease caused by strange microorganism of every sort (viruses and bacteria, etc.). More than 4 million people have died from the epidemic and at the time of writing, approximately 180 million people have acquired the infection of coronavirus [1]. The story of the COVID-19 outbreak began in Wuhan, China in December 2019. The outbreak spread very quickly to all parts of the world, and many people have been infected with COVID-19. The Italian Government issued an order on March 8, 2020 to close the borders of its country to reduce the spread of the epidemic in the country. The data were taken from the Center for Systems Science and Engineering (CSSE) at Johns Hopkins University, Baltimore, the United States [2]. These data were analyzed in a study to capture the period January 22, 2020 to March 15, 2020.

The recent COVID-19 pandemic is a respiratory system virus that is picked up by contact with an infectious man or woman through droplets in the air when a person coughs or sneezes or through small drops of saliva [3, 4]. People can also be infected by COVID-19 by touching a surface that is contaminated with the virus and then touching their face, especially their mouth or nose. The disease to appear in body takes 5 or 6 days and remain up to 14 days [5, 6]. By March 26, 2020 WHO declared it as pandemic. In the same time Chinees government had tried to control it. During 2020 Italy has been affected by COVID-19. Majority of COVID-19 cases in New York had been due to Europe not China [7]. On June

Methods of Mathematical Modeling. https://doi.org/10.1016/B978-0-323-99888-8.00001-2

11, 2020 several locally reported cases of COVID-19 were reported in USA [8]. On June 15, 2020 nearly 79 cases were reported in locality of Wuhan [9]. On June 29, 2020, the World Health Organization (WHO) warned people that transmission of this virus was still spreading increasingly as various countries reopened their businesses, although several countries were progressively decreasing the spread [10].

As of August 28, 2020, more than 24.4 million cases had been confirmed worldwide. More than 831,000 people had died from COVID-19 and more than 16 million people had recovered [2, 11, 12]. People fear COVID-19 because a similar disease before this killed more than 100,000 humans.Researchers and physicians try to suggest some precautionary measures for reducing the transmission of COVID. To know the fundamental causes for the COVID-19 pandemic, data of statistics and some mathematical formulations, concepts are needed. The idea of mathematical modeling was used first in 1927. The application of statistics data on different pandemics will contribute to the development of a mathematical model. This model will be used to model different real-world phenomena. Therefore, several real problems may be represented by one formula, as can be studied in [13–16]. So far, several scholars have analyzed the COVID-19 pandemic using some analytical methods as in [17–21]. Some of them have modeled the pandemic applying mathematical modeling that provides future predictions in light of the recent pandemic. The story, coupled with current information on such a disease, can help policy makers to build a few successful strategies for controlling it. Given the significance of mathematical modeling, the pandemic has been studied in many research articles [22–26]. Construction of mathematical models that involves parameters and various compartments which gives us information about transmission dynamics of infectious disease. As COVID-19 can spread easily in social situations, therefore some scholars have analyzed the dynamics of such a type of disease for transmission due to immigration as given here:

$$\begin{cases} \dot{\mathscr{S}} = \mathscr{S}(t)a - \mathscr{S}(t)b\mathscr{I}(t) + \mathscr{S}(t)e, \\ \dot{\mathscr{I}} = \mathscr{S}(t)b\mathscr{I}(t) + (-d - e + c)\mathscr{I}(t), \\ \mathscr{S}(0) = S_0, \ \ \mathscr{I}(0) = \mathscr{I}_0. \end{cases} \tag{1}$$

The mathematical models that we used in this chapter are inspired by the classic Lotka-Volterra model [27, 28] for analyzing predator-prey dynamics. The classic model has been suitably modified to build the susceptible-infected individual population dynamics model. The susceptible individual population is given by $\mathscr{S}(t)$ at time *t*. The infected individual population is given by $\mathscr{I}(t)$ at time *t*. The infection rate is given by $b = (1 - $*protection rate*$)$. The immigration rate of susceptible individuals is given by *a*. The immigration rate of infected individuals is given by *c*. The death rate is given by *d* and the recovered rate is given by *e*. Furthermore, the dynamics of COVID-19 epidemic models have been studied by several researchers for the numerical solution of COVID-19 models, and some methods have been introduced. In the last few years, several researchers used semianalytical techniques including the Sumudu decomposition method, Laplace Adomian decomposition method, the variation iteration method and many more from other sources; for numerical purposes, recent researchers used only the simple Euler method and the modified Euler method to handle the solution of the COVID-19 model. To the best of our knowledge, the Taylor's series method has not been applied yet to handle the solution of biological models in past decades. Therefore, we are now going to adopt the Taylor's series method to obtain the numerical solution of our new four compartmental integer-order model for COVID-19 given as

$$\begin{cases} \dfrac{\mathrm{d}\mathscr{S}(t)}{\mathrm{d}t} = -r\mathscr{S}(t)I(t), \\ \dfrac{\mathrm{d}I(t)}{\mathrm{d}t} = -r\mathscr{S}(t)I(t) - (a+d)I(t), \\ \dfrac{\mathrm{d}R(t)}{\mathrm{d}t} = aI(t), \\ \dfrac{\mathrm{d}D(t)}{\mathrm{d}t} = dI(t). \end{cases} \tag{2}$$

The given initial conditions are $\mathscr{S}(t_0) = \mathscr{S}_0$, $I\ (t_0) = I_0$, $R(t_0) = R_0$, and $D(t_0) = D_0$, r is the infection rate, a is the recovered rate, and d is the death rate due to infection. Therefore, in this chapter, we investigate a SIRD-type model for the numerical solution of COVID-19. We will use the Taylor's series method to find the appropriate solution of the above COVID-19 model. We will also investigate the fractional order of Eq. (2), as the fractional-order differential equation gives a more realistic result than that of the integer-order differential equation. The fraction-order equation for Eq. (2) is

$$\begin{cases} {}^{C}\mathrm{D}_t^{\wp}\mathscr{S}(t) = -r\mathscr{S}(t)I(t), \\ {}^{C}\mathrm{D}_t^{\wp}I(t) = r\mathscr{S}(t)I(t) - (a+d)I(t), \\ {}^{C}\mathrm{D}_t^{\wp}R(t) = aI(t), \\ {}^{C}\mathrm{D}_t^{\wp}D(t) = dI(t), \\ \mathscr{S}(t_0) = S_0, I(t_0) = I_0, \\ R(t_0) = R_0,\ D(t_0) = D_0, \end{cases} \tag{3}$$

where $0 < \wp \leq 1$.

The area of fractional calculus has received a great deal of attention in the last three decades. Renowned scientists have provided their contribution in this area by introducing different fractional operators in different articles. Modern calculus provides more realistic results compared to classical calculus. It describes the dynamics of different real-world phenomena lying between two integers. Furthermore, the fractional differential operators have greater degree of freedom and include the integer differential operators as special case. Up to now, various researchers have published many research articles, books, and different monographs which discuss the said area. Podlubny gave the physical and geometrical explanation of the fractional-order derivatives [29]. Analysis of various dynamical systems in the sense of fractional-order operators can be seen in [30–37]. The applications of this calculus in physics may be studied in [38]. Some fuzzy fractional-order linear and nonlinear dynamical problems have been analyzed for semianalytical solutions using the fractional Sumudo transform [39, 40]. Many types of publications have also been composed of existence, uniqueness, and numerical analysis under fractional-order concepts. The first notable definition was given by Riemann-Liouville in 1832. Then in 1967, this definition was modified by Caputo, and was mostly used to deal with various real-world problems. Recently in 2015, a new definition named the Caputo-Fabrizio (CF) derivative was provided by Caputo and Fabrizio by replacing the singular kernel in the previous definition with a nonsingular one. Later on, in 2016, Atangana, Baleanu, and Caputo further generalized the CF derivative to an ABC-type derivative. In our work, we will apply the Caputo fraction operator to our considered operator.

2 Fundamental results

In this section, we provide some fundamental lemmas and definitions from Refs. [29, 30, 41].

Definition 1. Let us present the arbitrary-order integral w.r.t τ as

$$ {}^{C}I_{\tau}^{\wp}\mathscr{S}(\tau)=\frac{1}{\Gamma(\wp)}\int_{0}^{\tau}(\tau-\eta)^{\wp-1}S(\eta)d\eta,\quad \wp>0, $$

where the integral on right-hand side converges.

Definition 2. Let us have an operator, say $\mathscr{S}(\tau)$; we give the Caputo fractional differentiation w.r.t τ as

$$ {}^{C}\mathrm{D}_{\tau}^{\wp}[\mathscr{S}(\tau)]=\frac{1}{\Gamma(n-\wp)}\int_{0}^{\tau}(\tau-\eta)^{n-\wp-1}\frac{d^{n}}{d\wp^{n}}[\mathscr{S}(\eta)]d\eta,\quad \wp>0, $$

with all operators are point-wise continuous on $\mathbf{R}_{+}$, $n=[\wp]+1$. If $\wp\in(0,1]$, then one has

$$ {}^{C}\mathrm{D}_{\tau}^{\wp}[\mathscr{S}(\tau)]=\frac{1}{\Gamma(1-\wp)}\int_{0}^{\tau}(\tau-\eta)^{-\wp}\frac{d}{d\wp}[\mathscr{S}(\eta)]d\eta. $$

Lemma 1. *Podlubny [29]. The solution of*

$$ {}^{C}\mathrm{D}_{\tau}^{\wp}\mathscr{S}(\tau)=X(\tau),\quad 0<\wp\leq 1 $$

is given by

$$ \mathscr{S}(\tau)=c_{0}+\frac{1}{\Gamma(1-\wp)}\int_{0}^{\tau}(\tau-\eta)^{\wp-1}X(\eta)d\eta. $$

Definition 3. The general Taylor's series mathematical expression for $g(t)$ is as follows:

$$ g(\tau)=\sum_{i=0}^{n}\frac{X^{i\wp}}{\Gamma(i\wp+1)}\mathrm{D}_{\tau}^{i\wp}g(0)+\frac{\mathrm{D}_{\tau}^{(n+1)\wp}g(\zeta)}{\Gamma((n+1)\wp+1)}, $$

with $0\leq\zeta\leq\tau$, $\forall\tau\in(0,a]$, $0<\wp\leq 1$. From this result, we can evaluate Euler's iterative technique.

Definition 4. Lipschitz conditions. Take a rectangular form R = (t, y):$a \le t \le b, c \le y \le d$ and consider that $f(t, y)$ is conditional on R. Then the operator f will fulfil the Lipschitzian condition in y on R for $L > 0$ and

$$|f(y,t) - f(\bar{y},t)| \le L^{*} |y - \bar{y}|, \quad (y,t),(\bar{y},t) \in \mathrm{R},$$

where L^* is called the Lipschitzian constant for f.

Theorem 1. *If* f (t, y) *is continuous on* R *then* $\exists$ L* > *0;* | f_y(t, y)| $\le$ L*, $\forall$ (t, y) $\in$*R. Then* f *fulfils the Lipschitzian condition in* y *with a Lipschitzian constant* L* *on R.*

Proof. Let t be fixed and $c \in (a, b)$, then

$$|f(t,y) - f(t,y_2)| = |f_y(t,c)(y_1 - y_2)|.$$

By using the mean value theorem, we satisfy

$$|(t,y) - f(t,y_2)| \le L^{*} |y_1 - y_2|. \qquad \square$$

.

Theorem 2. *Existence and uniqueness. Take* f (t, y) *as defined on R* = (t, y)*:*$t_0 \le$ b, c $\le$ y $\le$ d *if it satisfies L-condition on R in* y *and* (t_0, y_0) $\in$*R, then the IVP* y′ = f (t, y), y*(0)* = y_0 *has one solution on* $t_0 \le t_0 + \delta$.

Definition 5. Contraction operator. Consider an operator $T: X \to X$, where X is Banach space, then it is called contraction if for all $x, y \in X$, we have

$$|T_x - T_y| \le k|x - y|, \quad 0 < k < 1.$$

Theorem 3. *Banach contraction principle. In 1922, Banach stated that if T is a contraction operator on a Banach space* X *and let* D $\subseteq$ X *be a closed convex subset of* X *then* $T: X \to X$ *has a unique fixed point such that*

$$\| T_x - T_y \| \le k \| x - y \|,$$

for all $x, y \in D$, $0 < k < 1$.

Definition 6. Definition of Taylor's series. If a function $f(x)$ is such that $f(x), f'(x), f''(x)$, $f'''(x), \ldots, f^{n-1}(x)$ are said to be continuous on the closed interval $[x, x+h]$ and $f^n(x)$ exist in the open interval $(x, x + h)$ then there exists real number θ between 0 and 1 such that $f(x+h) = f(x) + hf'(x) + \frac{h^2}{2!}f''(x) + \frac{h^3}{3!}f'''(x) + \cdots + \frac{h^n}{n!}f^n(x + \theta h)$.

3 Feasibility of solution and stability analysis

Lemma 2. *The root of the proposed problem is bounded in the feasible region, provided as*

$$T = \{(S,I,R,D) \in R_+^4 : \quad 0 \le X(t) \le X_0\}$$

and the disease will occur if $\mathscr{S}_0 > \frac{a+d}{r}$.

Proof. Let

$$X(t) = \mathscr{S}(t) + I(t) + R(t) + D(t).$$

This implies that

$$\frac{X(t)}{dt}=\frac{\mathscr{S}(t)}{dt}+\frac{I(t)}{dt}+\frac{R(t)}{dt}+\frac{D(t)}{dt}.$$

On addition of all equations of Eq. (3), we obtain

$$\begin{aligned}\frac{dX}{dt} &= -r\mathscr{S}(t)I(t)+rI(t)\mathscr{S}(t)-(a+d)I(t)\\ &\quad +aI(t)+dI(t)\\ &=0.\end{aligned} \tag{4}$$

Evaluating Eq. (4), we have

$$\begin{aligned}X(t) &= X_0,\\ &= \mathscr{S}_0+I_0+R_0+D_0,\\ &= \mathscr{S}_0+I_0.\end{aligned}$$

This implies that $X(t)\leq X_0$. This derived the first part of the lemma.

Further, from the first equation of Eq. (3)

$$\frac{d\mathscr{S}}{dt}\leq 0$$

or

$$\mathscr{S}(t)\leq \mathscr{S}_0.$$

Therefore, $\mathscr{S}(t)$ is always decreasing and hence no disease will occur. From the second equation of Eq. (3) we have

$$\frac{dI(t)}{dt}=rI(t)\mathscr{S}(t)-(a+d)I(t),$$

$\frac{a+d}{r}$ is called the threshold phenomenon or critical community size for epidemic.

If

$$\mathscr{S}_0<\frac{a+d}{r}\Rightarrow\frac{dI(t)}{dt}<0,$$

then the infection class will decrease and hence no COVID-19 will occur. If

$$\mathscr{S}_0>\frac{a+d}{r}\Rightarrow\mathscr{S}(t)>\frac{a+d}{r}\Rightarrow\frac{dI(t)}{dt}>0,$$

then the infection class will increase and a pandemic will occur. By this we proved the second part of the lemma. □

Theorem 4. *The basic number of reproduction for Eq. (3) is computed as*

$$R_0=\frac{r}{a+d}\ \text{if}\ S\approx 1.$$

Proof. Let from second equation of Eq. (3) for computing the number of basic reproduction as $N=I$

$$\begin{aligned}{}^{C}\mathrm{D}_t^{\wp}(N) &= {}^{C}\mathrm{D}_t^{\wp}(I)=rI(t)S(t)-(a+d)I(t),\\ {}^{C}\mathrm{D}_t^{\wp}(N) &= F-V.\end{aligned}$$

Here $F = rI(t)\mathscr{S}(t)$, $V = (\gamma+\kappa)\Im(t)$, F is new infection, and V is the transferring of infection. Further, we calculate the matrix of next generation as FV^{-1}, where

$$F = \left[\frac{\partial}{\partial I}(rI(t)S(t))\right] = [r\mathscr{S}(t)]$$

and

$$V = \left[\frac{\partial}{\partial I}((a+d)I(t))\right] = [(a+d)], \quad V^{-1} = \left[\frac{1}{a+d}\right],$$

then

$$FV^{-1} = \left[\frac{rS}{(a+d)}\right].$$

Here R_0 is defined as the highest eigenvalue of the matrix of next generation FV^{-1}, as follows:

$$\begin{aligned} \rho(FV^{-1})_{E_0} &= \frac{rS}{(a+d)}, \\ R_0 &= \frac{rS_0}{(a+d)}, \end{aligned} \tag{5}$$

is the required reproduction number. Or if $\mathscr{S}(t) \approx 1$, then

$$R_0 = \frac{r}{a+d}.$$

Now as we know that $S_0 = \frac{a+d}{r}$, which leads us to $R_0 = 1$ having no meaning in biological terms, therefore, we can either take $S_0 < \frac{a+d}{r}$ for nonoccurrence of the pandemic or for disease-free equilibrium, $S_0 > \frac{a+d}{r}$ for the occurrence of a pandemic or for disease equilibrium point. This shows that

$$\begin{aligned} R_0 &< 1 \text{ for } S_0 < \frac{a+d}{r}, \\ R_0 &> 1 \text{ for } S_0 > \frac{a+d}{r}. \end{aligned}$$

□

Theorem 5. *System (3) will be locally asymptotically stable before a pandemic if*

$$R_0 < 1 \text{ for } S_0 < \frac{a+d}{r}$$

and locally asymptotically stable after a pandemic if

$$R_0 > 1 \text{ for } S_0 > \frac{a+d}{r}.$$

Proof. The proof of this theorem can be seen in Theorem 4. □

4 Qualitative analysis

In this section, we shall analyze some characteristics for the root of the fractional-order problem (3). The qualitative analysis of a problem is provided by fixed-point theory. Thus we use Banach and Schauder fixed-point theorems for the proof of the required results. We have considered the arbitrary-order model (3) as follows:

$$\begin{cases} {}^{C}\mathrm{D}_t^{\wp}\mathscr{S}(t) = \mho_1(t,\mathscr{S}(t),I(t),R(t),D(t)), \\ {}^{C}\mathrm{D}_t^{\wp}I(t) = \mho_2(t,\mathscr{S}(t),I(t),R(t),D(t)), \\ {}^{C}\mathrm{D}_t^{\wp}R(t) = \mho_3(t,\mathscr{S}(t),I(t),R(t),D(t)), \\ {}^{C}\mathrm{D}_t^{\wp}D(t) = \mho_4(t,\mathscr{S}(t),I(t),R(t),D(t)), \\ S(t_0) = S_0, I(t_0) = I_0, R(t_0) = R_0, D(t_0) = D_0, \\ 0 < \wp \le 1. \end{cases} \tag{6}$$

We apply an integral with order $\wp \in (0, 1]$ on Eq. (17), to get the nonlinear integral equations as follows:

$$\begin{aligned} S(t) &= S_0 + \frac{1}{\Gamma(\wp)}\int_0^t (t-\eta)^{\wp-1}\mho_1(\eta,S(\eta),I(\eta),R(\eta),D(\eta))d\eta, \\ I(t) &= I_0 + \frac{1}{\Gamma(\wp)}\int_0^t (t-\eta)^{\wp-1}\mho_2(\eta,S(\eta),I(\eta),R(\eta),D(\eta))d\eta, \\ R(t) &= R_0 + \frac{1}{\Gamma(\wp)}\int_0^t (t-\eta)^{\wp-1}\mho_3(\eta,S(\eta),I(\eta),R(\eta),D(\eta))d\eta, \\ D(t) &= D_0 + \frac{1}{\Gamma(\wp)}\int_0^t (t-\eta)^{\wp-1}\mho_4(\eta,S(\eta),I(\eta),R(\eta),D(\eta))d\eta. \end{aligned} \tag{7}$$

Next, taking $\infty > T \ge t \ge 0$, we have closed norm space by $E_1 = C([0, T] \times \mathbf{R}^4+, \mathbf{R}_+)$, clearly $E = E_1 \times E_2 \times E_3 \times E_4$ is also “closed norm space” having the norm

$$\| (S,I,R,\mathcal{D}) \| = \max_{t\in[0,T]} |\mathcal{S}(t)| + \max_{t\in[0,T]} |I(t) + \max_{t\in[0,T]} |R(t) + \max_{t\in[0,T]} |D(t)|.$$

We write system (16) as

$$F(t) = F_0(t) + \frac{1}{\Gamma(\wp)}\int_0^t (t-\eta)^{\wp-1}\psi(\eta,F(\eta))d\eta, \tag{8}$$

where

$$F(t) = \begin{cases} \mathcal{S}(t) \\ I(t) \\ R(t) \\ D(t) \end{cases}, \quad F_0(t) = \begin{cases} \mathcal{S}_0(t) \\ I_0(t) \\ R_0(t) \\ D_0(t) \end{cases} \tag{9}$$

and

$$\psi(t,F(t))=\begin{cases}\mho_1(t,\mathcal{S}(t),I(t),R(t),D(t))\\ \mho_2(t,\mathcal{S}(t),I(t),R(t),D(t))\\ \mho_3(t,\mathcal{S}(t),I(t),R(t),D(t))\\ \mho_4(t,\mathcal{S}(t),I(t),R(t),D(t))\end{cases}. \tag{10}$$

For derivation of existence and uniqueness, we take some growth conditions on mapping vector $\psi: [0,T]\times\mathbf{R}_+^4\to\mathbf{R}_+$ as follows:

($\boldsymbol{E}1$): There exist $L_\psi>0$ for all $F(t)$, $F(\bar{t})\in\mathbf{R}\times\mathbf{R}\times\mathbf{R}\times\mathbf{R}$;

$$|\psi(t,F(t))-\psi(t,F(\bar{t}))|\leq L_\psi|F(t)-F(\bar{t})|.$$

($\boldsymbol{E}2$): There exist $C_\psi>0$ and $M_\psi>0$;

$$|\psi(t,F(t))|\leq C_\psi|F|+M_\psi.$$

Theorem 6. *If* ψ *is continuous along with* $(E2)$, *problem* (3) *has at least one solution.*

Proof. Using the fixed-point theorem of Schauder, we have to prove the existence of a solution. We take a close subset C of E as

$$\mathbf{B}=\{F\in E:\ \|F\|\leq\mathbf{R},\ \mathbf{R}>0\}.$$

We take a mapping $\mathbf{B}: C\to C$ by Eq. (8) as

$$\mathbf{B}(F)=F_0(t)+\frac{1}{\Gamma(\wp)}\int_0^t(t-\eta)^{\wp-1}\psi(\eta,F(\eta))d\eta. \tag{11}$$

For any $F\in C$, we have

$$\begin{aligned}|\mathbf{B}(F)(t)|&\leq|F_0|+\frac{1}{\Gamma(\wp)}\int_0^t(t-\eta)^{\wp-1}|\psi(\eta,F(\eta))|d\eta\\&\leq|F_0|+\frac{1}{\Gamma(\wp)}\int_0^t(t-\eta)^{\wp-1}[C_\psi|F|+M_\psi]d\eta\\&\leq|F_0|+\frac{T^\wp}{\Gamma(\wp+1)}[C_\psi\|F\|+M_\psi],\end{aligned}$$

which implies that

$$\begin{aligned}\|\mathbf{B}(F)\|&\leq|F_0|+\frac{T^\wp}{\Gamma(\wp+1)}[C_\psi\|F\|+M_\psi]\\&\leq\mathbf{R}.\end{aligned} \tag{12}$$

Eq. (19) shows that $F\in C$. Thus $\mathbf{B}(C)\subset C$. This also shows that the mapping $\mathbf{B}$ has bounds. Next, for complete continuity, we go ahead as follows:

We take $t_2 > t_1 \in [0, T]$, then propose

$$\begin{aligned} |\mathbf{B}(F)(t_2)-\mathbf{B}(F)(t_1)| &= \left|\frac{1}{\Gamma(\wp)}\int_0^{t_2}(t_2-\eta)^{\wp-1},\psi(\eta,F(\eta))d\eta - \frac{1}{\Gamma(\wp)}\int_0^{t_1}(t_1-\eta)^{\wp-1}\psi(\eta,F(\eta))d\eta\right|, \\ &\leq \frac{1}{\Gamma(\wp)}\left[\int_0^{t_1}[(t_1-\eta)^{\wp-1}-(t_2-\eta)^{\wp-1}]\psi(\eta,F(\eta))d\eta \right. \\ &\quad \left. + \int_{t_1}^{t_2}(t_2-\eta)^{\eta-1}\psi(\eta,F(\eta))d\eta\right], \\ &\leq \frac{(C_\psi \mathbf{R}+M_\psi)}{\Gamma(\wp+1)}[t_2^\wp - t_1^\wp + 2(t_2-t_1)^\wp]. \end{aligned} \tag{13}$$

From Eq. (13), as t_1 approaches t_2, the right-hand side approaches to zero. So we conclude that

$$|\mathbf{B}(F)(t_2)-\mathbf{B}(F)(t_1)| \to 0, \text{ as } t_1 \to t_2.$$

Directly we say that

$$\| \mathbf{B}(F)(t_2)-\mathbf{B}(F)(t_1) \| \to 0, \text{ as } t_1 \to t_2.$$

Therefore, $\mathbf{B}$ is equi-continuous. By the Arzelá-Ascoli theorem, the mapping $\mathbf{B}$ is completely continuous and shown to be uniformly bounded. By Schauder's theorem, the given model (3) has at least one solution. □

Next we have to prove the uniqueness of solution as follows:

Theorem 7. *Under assumption* $(E1)$*, the considered problem (3) has one solution if* $\frac{T^\wp}{\Gamma(\wp+1)}L_\psi < 1$.

Proof. As $\mathbf{B}$: $E \to E$ given presection, we consider F and $\bar{F} \in E$ and proposed as

$$\begin{aligned} \| \mathbf{B}(F)-\mathbf{B}(\bar{F}) \| &= \sup_{t\in[0,T]}\left|\frac{1}{\Gamma(\wp)}\int_0^t (t-\eta)^{\wp-1}\psi(\eta,F(\eta))d\eta \right. \\ &\quad \left. -\frac{1}{\Gamma(\wp)}\int_0^t (t-\eta)^{\wp-1}\psi(\eta,\bar{F}(\eta))d\eta\right| \\ &\leq \frac{T^\wp}{\Gamma(\wp+1)}L_\psi \| F-\bar{F} \|. \end{aligned} \tag{14}$$

Eq. (14) implies

$$\| \mathbf{B}(F)-\mathbf{B}(\bar{F}) \| \leq \frac{T^\wp}{\Gamma(\wp+1)}L_\psi \| F-\bar{F} \|. \tag{15}$$

So $\mathbf{B}$ is contracted. Therefore, by the Banach contraction theorem, the proposed model has a unique solution. □

5 Series solution for model (2)

In this section, we will investigate the general solution and its numerical solution of the proposed COVID-19 model (2), by using the Taylor's series method.

5.1 General solution of COVID-19 model

For the general solution of the considered COVID-19 model (2), we will perform some steps:

Step 1: First of all we compute the first derivative of the $\mathcal{S}(t)$, $I(t)$, $R(t)$, and $D(t)$ as

$$\begin{cases} \mathcal{S}'(t_0) = -r\mathcal{S}_0 I_0, \\ I'(t_0) = r\mathcal{S}_0 I_0 - (a+d)I_0, \\ R'(t_0) = aI_0, \\ D'(t_0) = dI_0. \end{cases} \tag{16}$$

Step 2: We compute the second derivative of $\mathcal{S}(t)$, $I(t)$, $R(t)$, and $D(t)$ as

$$\begin{cases} \mathcal{S}''(t_0) = -r^2\mathcal{S}_0^2 I_0^2 + r\mathcal{S}_0 I_0(a+d) + r^2 I_0^2 \mathcal{S}_0, \\ I''(t_0) = r^2\mathcal{S}_0^2 I_0^2 - 2r\mathcal{S}_0 I_0(a+d) - r^2\mathcal{S}_0 I_0^2 + (a+d)^2 I_0, \\ R''(t_0) = ar\mathcal{S}_0 I_0 - a(a+d)I_0, \\ D''(t_0) = dr\mathcal{S}_0 I_0 - d(a+d)I_0. \end{cases} \tag{17}$$

Step 3: We compute the third derivative of $\mathcal{S}(t)$, $I(t)$, $R(t)$, and $D(t)$ as

$$\begin{cases} \mathcal{S}'''(t_0) = -r^3\mathcal{S}_0^3 I_0^3 + 2r^2\mathcal{S}_0^2 I_0(a+d) - r^4\mathcal{S}_0^2 I_0^3 - r^2\mathcal{S}_0 I_0^2(a+d) \\ \qquad -r\mathcal{S}_0 I_0(a+d)^2 - r^3\mathcal{S}_0 I_0^3 + r^4\mathcal{S}_0^3 I_0 + r^2\mathcal{S}_0 I_0^2(a+d)^2 - 2r^2\mathcal{S}_0^2 I_0^2(a+d), \\ I'''(t_0) = 2r^3\mathcal{S}_0^3 I_0 - 2r^2\mathcal{S}_0^2 I_0^2(a+d) - 2r^3\mathcal{S}_0^2 I_0^3 - r^2\mathcal{S}_0^2 I_0(a+d) \\ \qquad + r\mathcal{S}_0 I_0(a+d)^2 + r^2 I_0^2\mathcal{S}_0(a+d) - 2r^3\mathcal{S}_0^2 I_0^2 + 2r^2\mathcal{S}_0 I_0^2 + r^2 I_0^3\mathcal{S}_0 - r^2\mathcal{S}_0^2 I_0 \\ \qquad + r\mathcal{S}_0 I_0(a+d) + r^2\mathcal{S}_0 I_0^2(a+d) + r\mathcal{S}_0 I_0(a+d)^2 - I_0(a+d)^3, \\ R'''(t_0) = ar^2\mathcal{S}_0^2 I_0 - 2a(a+d)r\mathcal{S}_0 I_0 - ar^2\mathcal{S}_0 I_0^2 + a(a+d)^2 I_0, \\ D'''(t_0) = dr^2\mathcal{S}_0^2 I_0 - 2d(a+d)r\mathcal{S}_0 I_0 - dr^2\mathcal{S}_0 I_0^2 + d(a+d)^2 I_0. \end{cases} \tag{18}$$

Step 4: We compute the fourth derivative of $\mathcal{S}(t), I(t), R(t)$, and $D(t)$ as

$$
\begin{cases}
\begin{aligned}
\mathcal{S}^{iv}(t_0) = {} & -r\mathcal{S}_0^4 I_0^4 + (a+d) r^3 \mathcal{S}_0^3 I_0 + 3rI_0^2\mathcal{S}_0^3 + r^3(a+d)\mathcal{S}_0^3 I_0 \\
& - r^2(a+d)\mathcal{S}_0^2 I_0 - 2r^3(a+d) I_0^2 \mathcal{S}_0^2 - 3r^5\mathcal{S}_0^3 I_0^3 + 3r^4(a+d)\mathcal{S}_0^2 I_0^3 \\
& + 2r^5 I_0^4 \mathcal{S}_0^2 + r^3(a+d)\mathcal{S}_0^3 I_0 - r^2(a+d)^2\mathcal{S}_0^2 I_0 - 2r^3 I_0^2\mathcal{S}_0^2 - r^3(a+d)^2\mathcal{S}_0^2 I_0 \\
& + r(a+d)^3\mathcal{S}_0 I_0 + r^2(a+d)^2\mathcal{S}_0 I_0^2 - 2r^3(a+d)\mathcal{S}_0^2 I_0^2 + 2r^2(a+d)^2\mathcal{S}_0 I_0^2 \\
& + r^3(a+d)\mathcal{S}_0 I_0^3 - 3r^4\mathcal{S}_0^2 I_0^3 + 3r^3(a+d)\mathcal{S}_0 I_0^3 + r^4 I_0^4\mathcal{S}_0 + 2r^5\mathcal{S}_0^4 I_0^2 \\
& - 2r^4(a+d)\mathcal{S}_0^3 I_0^2 - 3r^5 I_0^3\mathcal{S}_0^2 + 2r^3(a+d)^2\mathcal{S}_0^2 I_0 - 2r^2(a+d)^3\mathcal{S}_0 I_0^2 \\
& - r^3(a+d)^3\mathcal{S}_0 I_0^3 - 4r^2(a+d)\mathcal{S}_0^3 I_0^2 + 4r^3(a+d)^2\mathcal{S}_0^2 I_0^2 + 4r^3(a+d)\mathcal{S}_0^2 I_0^3, \\
I^{iv}(t_0) = {} & 2r^4\mathcal{S}_0^4 I_0 - 2r^3(a+d)\mathcal{S}_0^3 I_0 - 6r^4\mathcal{S}_0^2 I_0^2 - 4(a+d)r^3\mathcal{S}_0^3 I_0^2 \\
& + 4(a+d)^2 r^2\mathcal{S}_0^2 I_0^2 + 7r^3 I_0^3\mathcal{S}_0^2 - 6r^4\mathcal{S}_0^3 I_0^2 + 6r^3(a+d)\mathcal{S}_0^2 I_0^3 \\
& + 4r^4 I_0^4\mathcal{S}_0^2 - r^3(a+d) I_0\mathcal{S}_0^3 + 2r^2(a+d)^2\mathcal{S}_0^2 I_0 + 2r^3\mathcal{S}_0^2 I_0^2 + r(a+d)^2\mathcal{S}_0^2 I_0 \\
& - 3r(a+d)^3\mathcal{S}_0 I_0 - 6r^2(a+d)^2\mathcal{S}_0 I_0^2 - 2r^3(a+d)\mathcal{S}_0 I_0^3 + 4r^3(a+d)\mathcal{S}_0^2 I_0^2 \\
& - 4r^4\mathcal{S}_0^3 I_0^2 + 4r^3(a+d)\mathcal{S}_0^2 I_0^2 + 4r^4 I_0^3\mathcal{S}_0^2 + 4r^3\mathcal{S}_0^2 I_0^2 - 4r^2(a+d)\mathcal{S}_0 I_0^2 \\
& - 2r^3\mathcal{S}_0 I_0^3 - r^3\mathcal{S}_0 I_0^4 - 3r^2(a+d)\mathcal{S}_0 I_0^3 - r^3\mathcal{S}_0^3 I_0 + r^2(a+d)\mathcal{S}_0^2 I_0 \\
& + 2r^3\mathcal{S}_0^2 I_0^2 + r^2(a+d)\mathcal{S}_0^2 I_0 - r(a+d)\mathcal{S}_0 I_0 - r(a+d)\mathcal{S}_0 I_0^2 + (a+d)^4 I_0, \\
R^{iv}(t_0) = {} & ar^3\mathcal{S}_0^3 I_0 - 3a(a+d)r^2\mathcal{S}_0^2 I_0 - 4ar^3 I_0^2\mathcal{S}_0^2 + 3a(a+d)^2 r\mathcal{S}_0 I_0 \\
& + 4a(a+d)r^2 I_0^2\mathcal{S}_0 + ar^3\mathcal{S}_0 I_0^3 - a(a+d)^3 I_0, \\
D^{iv}(t_0) = {} & dr^3\mathcal{S}_0^3 I_0 - 3d(a+d)r^2\mathcal{S}_0^2 I_0 - 4dr^3 I_0^2\mathcal{S}_0^2 + 3d(a+d)^2 r\mathcal{S}_0 I_0 \\
& + 4d(a+d)r^2 I_0^2\mathcal{S}_0 + dr^3\mathcal{S}_0 I_0^3 - d(a+d)^3 I_0.
\end{aligned}
\end{cases}
\tag{19}
$$

Step 5: We compute the fifth derivative of $\mathcal{S}(t)$, $I(t)$, $R(t)$, and $D(t)$ as

$$\begin{cases}
\mathcal{S}^{v}(t_0)=-r^5\mathcal{S}_0^5I_0^5+4r^4(a+d)\mathcal{S}_0^4I_0+4r^4\mathcal{S}_0^5I_0^5-4r^3(a+d)\mathcal{S}_0^4I_0^2\\
\qquad -5r^3(a+d)^2\mathcal{S}_0^3I_0-17r^4(a+d)\mathcal{S}_0^3I_0^2-9r^2\mathcal{S}_0^3I_0^3+6r^2\mathcal{S}_0^4I_0^2\\
\qquad -6r(a+d)\mathcal{S}_0^3I_0^2+3r^2(a+d)\mathcal{S}_0^3I_0+14r^3(a+d)^2\mathcal{S}_0^2I_0^2-17r^6\mathcal{S}_0^4I_0^3\\
\qquad +36r^5(a+d)\mathcal{S}_0^3I_0^3+17r^6\mathcal{S}_0^3I_0^4-24(a+d)^2r^4\mathcal{S}_0^2I_0^3-6(a+d)r^5\mathcal{S}_0^2I_0^2\\
\qquad -4r^6\mathcal{S}_0^2I_0^5-8r^5(a+d)\mathcal{S}_0^2I_0^4+4r^4I_0^3\mathcal{S}_0^2-4r^4\mathcal{S}_0^3I_0^2+4r^3(a+d)\mathcal{S}_0^2I_0^2\\
\qquad -r^4(a+d)^2\mathcal{S}_0^3I_0+r^3(a+d)^3\mathcal{S}_0^2I_0+2r^4(a+d)^2\mathcal{S}_0^2I_0^2\\
\qquad -r(a+d)^4\mathcal{S}_0I_0-3r^2(a+d)^3I_0^2\mathcal{S}_0+26r^4(a+d)\mathcal{S}_0^2I_0^3\\
\qquad -4r^2(a+d)^3\mathcal{S}_0I_0^2-14r^3(a+d)^2\mathcal{S}_0I_0^3-4r^4(a+d)\mathcal{S}_0I_0^4-9r^5\mathcal{S}_0^3I_0^3\\
\qquad +6r^5I_0^4\mathcal{S}_0^2-r^5\mathcal{S}_0I_0^2-4r^5\mathcal{S}_0^5I_0+4r^6\mathcal{S}_0^5I_0^2-16r^5(a+d)\mathcal{S}_0^4I_0^4\\
\qquad +24r^4(a+d)^2\mathcal{S}_0^3I_0^2+6r^6I_0^4\mathcal{S}_0^2-9r^6\mathcal{S}_0^3I_0^3+9r^5(a+d)\mathcal{S}_0^2I_0^3\\
\qquad -12r^3(a+d)^2\mathcal{S}_0^3I_0^3+r^4(a+d)^2\mathcal{S}_0I_0^4+3r^3(a+d)^3\mathcal{S}_0I_0^3+12r^4(a+d)\mathcal{S}_0^3I_0^3\\
\qquad -12r^3(a+d)^2\mathcal{S}_0^2I_0^3-8r^4(a+d)I_0^4\mathcal{S}_0^2,\\
I^{v}(t_0)=2r^5\mathcal{S}_0^5I_0-4(a+d)r^4\mathcal{S}_0^4I_0-28r^5\mathcal{S}_0^4I_0^2+4(a+d)^2r^3\mathcal{S}_0^3I_0\\
\qquad +37(a+d)r^4\mathcal{S}_0^3I_0^2+42r^5\mathcal{S}_0^3I_0^3-8(a+d)r^4\mathcal{S}_0^4I_0^2+16(a+d)^2r^3\mathcal{S}_0^3I_0^2\\
\qquad +38(a+d)r^4\mathcal{S}_0^3I_0^3-8(a+d)^3r^2\mathcal{S}_0^2I_0^2-8(a+d)^2r^3I_0^3\mathcal{S}_0^2-18r^4\mathcal{S}_0^2I_0^4\\
\qquad +21r^4\mathcal{S}_0^3I_0^3-12(a+d)r^3I_0^3\mathcal{S}_0^2-18r^5\mathcal{S}_0^4I_0^3+18r^5I_0^4\mathcal{S}_0^4\\
\qquad +18(a+d)^2r^3I_0^3\mathcal{S}_0-28(a+d)r^4I_0^4\mathcal{S}_0^2-(a+d)r^4\mathcal{S}_0^4I_0+2(a+d)r^3\mathcal{S}_0^3I_0\\
\qquad -4(a+d)r^2\mathcal{S}_0^2I_0-33(a+d)^2r^3\mathcal{S}_0^2I_0^2-30(a+d)r^3\mathcal{S}_0^2I_0^2-14r^4I_0^3\mathcal{S}_0^2\\
\qquad +r^2(a+d)\mathcal{S}_0^3I_0-r(a+d)^3\mathcal{S}_0^2I_0-r^2(a+d)^2\mathcal{S}_0^2I_0+3(a+d)^4r\mathcal{S}_0I_0\\
\qquad +15(a+d)^3r^2\mathcal{S}_0I_0^2+23(a+d)r^3\mathcal{S}_0I_0^3-30(a+d)r^4\mathcal{S}_0^2I_0^3+r^4(a+d)^2I_0^4\mathcal{S}_0\\
\qquad -8r^5\mathcal{S}_0^2I_0^4+8r^3\mathcal{S}_0^3I_0^2+11(a+d)^2r^2\mathcal{S}_0I_0^2+2r^4I_0^4\mathcal{S}_0+4r^3(a+d)\mathcal{S}_0I_0^4\\
\qquad +r^4\mathcal{S}_0I_0^5+9(a+d)^2r^2\mathcal{S}_0I_0^3+r^4(a+d)\mathcal{S}_0I_0^4+r(a+d)^4\mathcal{S}_0I_0-(a+d)^5I_0,\\
R^{v}(t_0)=ar^4\mathcal{S}_0^4I_0-4a(a+d)r^3\mathcal{S}_0^3I_0-11ar^4\mathcal{S}_0^3I_0^2+20a(a+d)r^3\mathcal{S}_0^2I_0^2\\
\qquad +6a(a+d)^2r^2\mathcal{S}_0^2I_0+11ar^4\mathcal{S}_0^2I_0^3-4a(a+d)^3r\mathcal{S}_0I_0-11a(a+d)^2\mathcal{S}_0I_0^2r^2\\
\qquad -7a(a+d)r^3\mathcal{S}_0I_0^3-ar^4\mathcal{S}_0I_0^4+a(a+d)^4I_0,\\
D^{v}(t_0)=dr^4\mathcal{S}_0^4I_0-4d(a+d)r^3\mathcal{S}_0^3I_0-11dr^4\mathcal{S}_0^3I_0^2+20d(a+d)r^3\mathcal{S}_0^2I_0^2\\
\qquad +6d(a+d)^2r^2\mathcal{S}_0^2I_0+11dr^4\mathcal{S}_0^2I_0^3-4d(a+d)^3r\mathcal{S}_0I_0-11d(a+d)^2\mathcal{S}_0I_0^2r^2\\
\qquad -7d(a+d)r^3\mathcal{S}_0I_0^3-dr^4\mathcal{S}_0I_0^4+d(a+d)^4I_0.
\end{cases} \tag{20}$$

Now the solution for the first six terms is given by

$$
\begin{cases}
\mathcal{S}(t)=\mathcal{S}(t_0)+t\mathcal{S}^{'}(t_0)+t^2\dfrac{\mathcal{S}^{''}(t_0)}{2!}+t^3\dfrac{\mathcal{S}^{'''}(t_0)}{3!}+t^4\dfrac{\mathcal{S}^{iv}(t_0)}{4!}+t^5\dfrac{\mathcal{S}^{v}(t_0)}{5!}+\cdots,\\
I(t)=I(t_0)+tI^{'}(t_0)+t^2\dfrac{I^{''}(t_0)}{2!}+t^3\dfrac{I^{'''}(t_0)}{3!}+t^4\dfrac{I^{iv}(t_0)}{4!}+t^5\dfrac{I^{v}(t_0)}{5!}+\cdots,\\
R(t)=R(t_0)+tR^{'}(t_0)+t^2\dfrac{R^{''}(t_0)}{2!}+t^3\dfrac{R^{'''}(t_0)}{3!}+t^4\dfrac{R^{iv}(t_0)}{4!}+t^5\dfrac{R^{v}(t_0)}{5!}+\cdots,\\
D(t)=D(t_0)+tD^{'}(t_0)+t^2\dfrac{D^{''}(t_0)}{2!}+t^3\dfrac{D^{'''}(t_0)}{3!}+t^4\dfrac{D^{iv}(t_0)}{4!}+t^5\dfrac{D^{v}(t_0)}{5!}+\cdots.
\end{cases}
\tag{21}
$$

Substituting the values of Eqs. (3), (17)–(20) in Eq. (21), we have

$$
\begin{cases}
\mathcal{S}(t)=\mathcal{S}(t_0)+t[-r\mathcal{S}_0I_0]+\dfrac{t^2}{2!}[-r^2\mathcal{S}_0^2I_0^2+r\mathcal{S}_0I_0(a+d)+r^2I_0^2\mathcal{S}_0]\\
\qquad+\dfrac{t^3}{3!}[-r^3\mathcal{S}_0^3I_0^3+2r^2\mathcal{S}_0^2I_0(a+d)-r^4\mathcal{S}_0^2I_0^3-r^2\mathcal{S}_0I_0^2(a+d)\\
\qquad-r\mathcal{S}_0I_0(a+d)^2-r^3\mathcal{S}_0I_0^3+r^4\mathcal{S}_0^3I_0+r^2\mathcal{S}_0I_0^2(a+d)^2-2r^2\mathcal{S}_0^2I_0^2(a+d)]\\
\qquad+\dfrac{t^4}{4!}[-r\mathcal{S}_0^4I_0^4+(a+d)r^3\mathcal{S}_0^3I_0+3rI_0^2\mathcal{S}_0^3+r^3(a+d)\mathcal{S}_0^3I_0\\
\qquad-r^2(a+d)\mathcal{S}_0^2I_0-2r^3(a+d)I_0^2\mathcal{S}_0^2-3r^5\mathcal{S}_0^3I_0^3+3r^4(a+d)\mathcal{S}_0^2I_0^3\\
\qquad+2r^5I_0^4\mathcal{S}_0^2+r^3(a+d)\mathcal{S}_0^3I_0-r^2(a+d)^2\mathcal{S}_0^2I_0-2r^3I_0^2\mathcal{S}_0^2-r^3(a+d)^2\mathcal{S}_0^2I_0\\
\qquad+r(a+d)^3\mathcal{S}_0I_0+r^2(a+d)^2\mathcal{S}_0I_0^2-2r^3(a+d)\mathcal{S}_0^2I_0^2+2r^2(a+d)^2\mathcal{S}_0I_0^2\\
\qquad+r^3(a+d)\mathcal{S}_0I_0^3-3r^4\mathcal{S}_0^2I_0^3+3r^3(a+d)\mathcal{S}_0I_0^3+r^4I_0^4\mathcal{S}_0+2r^5\mathcal{S}_0^4I_0^2\\
\qquad-2r^4(a+d)\mathcal{S}_0^3I_0^2-3r^5I_0^3\mathcal{S}_0^2+2r^3(a+d)^2\mathcal{S}_0^2I_0-2r^2(a+d)^3\mathcal{S}_0I_0^2\\
\qquad-r^3(a+d)^3\mathcal{S}_0I_0^3-4r^2(a+d)\mathcal{S}_0^3I_0^2+4r^3(a+d)^2\mathcal{S}_0^2I_0^2+4r^3(a+d)\mathcal{S}_0^2I_0^3]\\
\qquad+\dfrac{t^5}{5!}[-r^5\mathcal{S}_0^5I_0^5+4r^4(a+d)\mathcal{S}_0^4I_0+4r^4\mathcal{S}_0^5I_0^5\\
\qquad-4r^3(a+d)\mathcal{S}_0^4I_0^2-5r^3(a+d)^2\mathcal{S}_0^3I_0-17r^4(a+d)\mathcal{S}_0^3I_0^2-9r^2\mathcal{S}_0^3I_0^3\\
\qquad+6r^2\mathcal{S}_0^4I_0^2-6r(a+d)\mathcal{S}_0^3I_0^2+3r^2(a+d)\mathcal{S}_0^3I_0+14r^3(a+d)^2\mathcal{S}_0^2I_0^2\\
\qquad-17r^6\mathcal{S}_0^4I_0^3+36r^5(a+d)\mathcal{S}_0^3I_0^3+17r^6\mathcal{S}_0^3I_0^4-24(a+d)^2r^4\mathcal{S}_0^2I_0^3\\
\qquad-6(a+d)r^5\mathcal{S}_0^2I_0^2-4r^6\mathcal{S}_0^2I_0^5-8r^5(a+d)\mathcal{S}_0^2I_0^4+4r^4I_0^3\mathcal{S}_0^2\\
\qquad-4r^4\mathcal{S}_0^3I_0^2+4r^3(a+d)\mathcal{S}_0^2I_0^2-r^4(a+d)^2\mathcal{S}_0^3I_0+r^3(a+d)^3\mathcal{S}_0^2I_0\\
\qquad+2r^4(a+d)^2\mathcal{S}_0^2I_0^2-r(a+d)^4\mathcal{S}_0I_0-3r^2(a+d)^3I_0^2\mathcal{S}_0+26r^4(a+d)\mathcal{S}_0^2I_0^3\\
\qquad-4r^2(a+d)^3\mathcal{S}_0I_0^2-14r^3(a+d)^2\mathcal{S}_0I_0^3-4r^4(a+d)\mathcal{S}_0I_0^4-9r^5\mathcal{S}_0^3I_0^3\\
\qquad+6r^5I_0^4\mathcal{S}_0^2-r^5\mathcal{S}_0I_0^2-4r^5\mathcal{S}_0^5I_0+4r^6\mathcal{S}_0^5I_0^2-16r^5(a+d)\mathcal{S}_0^4I_0^4\\
\qquad+24r^4(a+d)^2\mathcal{S}_0^3I_0^2+6r^6I_0^4\mathcal{S}_0^2-9r^6\mathcal{S}_0^3I_0^3+9r^5(a+d)\mathcal{S}_0^2I_0^3\\
\qquad-12r^3(a+d)^2\mathcal{S}_0^3I_0^3+r^4(a+d)^2\mathcal{S}_0I_0^4+3r^3(a+d)^3\mathcal{S}_0I_0^3+12r^4(a+d)\mathcal{S}_0^3I_0^3\\
\qquad-12r^3(a+d)^2\mathcal{S}_0^2I_0^3-8r^4(a+d)I_0^4\mathcal{S}_0^2]+\cdots,
\end{cases}
\tag{22}
$$

$$
\left\{
\begin{aligned}
I(t) = {} & I(t_0) + t[r\mathcal{S}_0 I_0 - (a+d)I_0] + \frac{t^2}{2!}[r^2\mathcal{S}_0^2 I_0^2 - 2r\mathcal{S}_0 I_0(a+d) - r^2\mathcal{S}_0 I_0^2 \\
& + (a+d)^2 I_0] + \frac{t^3}{3!}[2r^3\mathcal{S}_0^3 I_0 - 2r^2\mathcal{S}_0^2 I_0^2(a+d) - 2r^3\mathcal{S}_0^2 I_0^3 - r^2\mathcal{S}_0^2 I_0(a+d) \\
& + r\mathcal{S}_0 I_0(a+d)^2 + r^2 I_0^2\mathcal{S}_0(a+d) - 2r^3\mathcal{S}_0^2 I_0^2 + 2r^2\mathcal{S}_0 I_0^2 + r^2 I_0^3\mathcal{S}_0 \\
& - r^2\mathcal{S}_0^2 I_0 + r\mathcal{S}_0 I_0(a+d) + r^2\mathcal{S}_0 I_0^2(a+d) + r\mathcal{S}_0 I_0(a+d)^2 - I_0(a+d)^3] \\
& + \frac{t^4}{4!}[2r^4\mathcal{S}_0^4 I_0 - 2r^3(a+d)\mathcal{S}_0^3 I_0 - 6r^4\mathcal{S}_0^2 I_0^2 - 4(a+d)r^3\mathcal{S}_0^3 I_0^2 \\
& + 4(a+d)^2 r^2\mathcal{S}_0^2 I_0^2 + 7r^3 I_0^3\mathcal{S}_0^2 - 6r^4\mathcal{S}_0^3 I_0^2 + 6r^3(a+d)\mathcal{S}_0^2 I_0^3 \\
& + 4r^4 I_0^4\mathcal{S}_0^2 - r^3(a+d)I_0\mathcal{S}_0^3 + 2r^2(a+d)^2\mathcal{S}_0^2 I_0 + 2r^3\mathcal{S}_0^2 I_0^2 + r(a+d)^2\mathcal{S}_0^2 I_0 \\
& - 3r(a+d)^3\mathcal{S}_0 I_0 - 6r^2(a+d)^2\mathcal{S}_0 I_0^2 - 2r^3(a+d)\mathcal{S}_0 I_0^3 + 4r^3(a+d)\mathcal{S}_0^2 I_0^2 \\
& - 4r^4\mathcal{S}_0^3 I_0^2 + 4r^3(a+d)\mathcal{S}_0^2 I_0^2 + 4r^4 I_0^3\mathcal{S}_0^2 + 4r^3\mathcal{S}_0^2 I_0^2 - 4r^2(a+d)\mathcal{S}_0 I_0^2 \\
& - 2r^3\mathcal{S}_0 I_0^3 - r^3\mathcal{S}_0 I_0^4 - 3r^2(a+d)\mathcal{S}_0 I_0^3 - r^3\mathcal{S}_0^3 I_0 + r^2(a+d)\mathcal{S}_0^2 I_0 \\
& + 2r^3\mathcal{S}_0^2 I_0^2 + r^2(a+d)\mathcal{S}_0^2 I_0 - r(a+d)\mathcal{S}_0 I_0 - r(a+d)\mathcal{S}_0 I_0^2 \\
& + (a+d)^4 I_0] + \frac{t^5}{5!}[2r^5\mathcal{S}_0^5 I_0 - 4(a+d)r^4\mathcal{S}_0^4 I_0 - 28r^5\mathcal{S}_0^4 I_0^2 \\
& + 4(a+d)^2 r^3\mathcal{S}_0^3 I_0 + 37(a+d)r^4\mathcal{S}_0^3 I_0^2 + 42r^5\mathcal{S}_0^3 I_0^3 - 8(a+d)r^4\mathcal{S}_0^4 I_0^2 \\
& + 16(a+d)^2 r^3\mathcal{S}_0^3 I_0^2 + 38(a+d)r^4\mathcal{S}_0^3 I_0^3 - 8(a+d)^3 r^2\mathcal{S}_0^2 I_0^2 \\
& - 8(a+d)^2 r^3 I_0^3\mathcal{S}_0^2 - 18r^4\mathcal{S}_0^2 I_0^4 + 21r^4\mathcal{S}_0^3 I_0^3 - 12(a+d)r^3 I_0^3\mathcal{S}_0^2 \\
& - 18r^5\mathcal{S}_0^4 I_0^3 + 18r^5 I_0^4\mathcal{S}_0^4 + 18(a+d)^2 r^3 I_0^3\mathcal{S}_0 - 28(a+d)r^4 I_0^4\mathcal{S}_0^2 \\
& - (a+d)r^4\mathcal{S}_0^4 I_0 + 2(a+d)r^3\mathcal{S}_0^3 I_0 - 4(a+d)r^2\mathcal{S}_0^2 I_0 - 33(a+d)^2 r^3\mathcal{S}_0^2 I_0^2 \\
& - 30(a+d)r^3\mathcal{S}_0^2 I_0^2 - 14r^4 I_0^3\mathcal{S}_0^2 + r^2(a+d)\mathcal{S}_0^3 I_0 - r(a+d)^3\mathcal{S}_0^2 I_0 \\
& - r^2(a+d)^2\mathcal{S}_0^2 I_0 + 3(a+d)^4 r\mathcal{S}_0 I_0 + 15(a+d)^3 r^2\mathcal{S}_0 I_0^2 + 23(a+d)r^3\mathcal{S}_0 I_0^3 \\
& - 30(a+d)r^4\mathcal{S}_0^2 I_0^3 + r^4(a+d)^2 I_0^4\mathcal{S}_0 - 8r^5\mathcal{S}_0^2 I_0^4 + 8r^3\mathcal{S}_0^3 I_0^2 \\
& + 11(a+d)^2 r^2\mathcal{S}_0 I_0^2 + 2r^4 I_0^4\mathcal{S}_0 + 4r^3(a+d)\mathcal{S}_0 I_0^4 + r^4\mathcal{S}_0 I_0^5 + 9(a+d)^2 r^2\mathcal{S}_0 I_0^3 \\
& + r^4(a+d)\mathcal{S}_0 I_0^4 + r(a+d)^4\mathcal{S}_0 I_0 - (a+d)^5 I_0] + \cdots,
\end{aligned}
\right. \tag{23}
$$

$$\begin{cases} R(t) = R(t_0) + t[aI_0] + \dfrac{t^2}{2!}[ar\mathcal{S}_0I_0 - a(a+d)I_0] + \dfrac{t^3}{3!}[ar^2\mathcal{S}_0^2I_0 \\ \qquad -2a(a+d)r\mathcal{S}_0I_0 - ar^2\mathcal{S}_0I_0^2 + a(a+d)^2I_0] + \dfrac{t^4}{4!}[ar^3\mathcal{S}_0^3I_0 \\ \qquad -3a(a+d)r^2\mathcal{S}_0^2I_0 - 4ar^3I_0^2\mathcal{S}_0^2 + 3a(a+d)^2r\mathcal{S}_0I_0 + 4a(a+d)r^2I_0^2\mathcal{S}_0 \\ \qquad + ar^3\mathcal{S}_0I_0^3 - a(a+d)^3I_0] + \dfrac{t^5}{5!}[ar^4\mathcal{S}_0^4I_0 - 4a(a+d)r^3\mathcal{S}_0^3I_0 \\ \qquad -11ar^4\mathcal{S}_0^3I_0^2 + 20a(a+d)r^3\mathcal{S}_0^2I_0^2 + 6a(a+d)^2r^2\mathcal{S}_0^2I_0 + 11ar^4\mathcal{S}_0^2I_0^3 \\ \qquad -4a(a+d)^3r\mathcal{S}_0I_0 - 11a(a+d)^2\mathcal{S}_0I_0^2r^2 \\ \qquad -7a(a+d)r^3\mathcal{S}_0I_0^3 - ar^4\mathcal{S}_0I_0^4 + a(a+d)^4I_0] + \cdots, \\ D(t) = D(t_0) + t[dI_0] + \dfrac{t^2}{2!}[dr\mathcal{S}_0I_0 - d(a+d)I_0] + \dfrac{t^3}{3!}[dr^2\mathcal{S}_0^2I_0 \\ \qquad -2d(a+d)r\mathcal{S}_0I_0 - dr^2\mathcal{S}_0I_0^2 + d(a+d)^2I_0] + \dfrac{t^4}{4!}[dr^3\mathcal{S}_0^3I_0 \\ \qquad -3d(a+d)r^2S_0^2I_0 - 4dr^3I_0^2S_0^2 + 3d(a+d)^2rS_0I_0 + 4d(a+d)r^2I_0^2S_0 \\ \qquad + dr^3\mathcal{S}_0I_0^3 - d(a+d)^3I_0] + \dfrac{t^5}{5!}[dr^4\mathcal{S}_0^4I_0 - 4d(a+d)r^3\mathcal{S}_0^3I_0 \\ \qquad -11dr^4\mathcal{S}_0^3I_0^2 + 20d(a+d)r^3\mathcal{S}_0^2I_0^2 + 6d(a+d)^2r^2\mathcal{S}_0^2I_0 + 11dr^4\mathcal{S}_0^2I_0^3 \\ \qquad -4d(a+d)^3r\mathcal{S}_0I_0 - 11d(a+d)^2\mathcal{S}_0I_0^2r^2 - 7d(a+d)r^3\mathcal{S}_0I_0^3 \\ \qquad -dr^4\mathcal{S}_0I_0^4 + d(a+d)^4I_0] + \cdots. \end{cases} \tag{24}$$

6 Numerical solution for Eq. (3)

In this section, we have to calculate numerical result of the Caputo arbitrary-order problem (3) and the presentation of iterative simulations will be established by the proposed Euler's or Taylor's series iterative method. To achieve this, we apply the fractional-order Caputo differentiation to get an approximate scheme for the graphical representation of our chosen problem (3). To construct an approximate procedure, we go further with the process for Eq. (3) as

$$\begin{cases} {}^{C}\mathrm{D}_t^{\wp}\mathcal{S}(t) = \mho_1(t,\mathcal{S}(t),I(t),R(t),D(t)) = -r\mathcal{S}(t)I(t), \\ {}^{C}\mathrm{D}_t^{\wp}I(t) = \mho_2(t,\mathcal{S}(t),I(t),R(t),D(t)) = -r\mathcal{S}(t)I(t) - (a+d)I(t), \\ {}^{C}\mathrm{D}_t^{\wp}R(t) = \mho_3(t,\mathcal{S}(t),I(t),R(t),D(t)) = aI(t), \\ {}^{C}\mathrm{D}_t^{\wp}D(t) = \mho_4(t,\mathcal{S}(t),I(t),R(t),D(t)) = dI(t), \\ \mathcal{S}(0) = S_0, \quad I(0) = I_0,\ 0 < \theta \le 1,\ t > 0. \end{cases} \tag{25}$$

Let $[0, \wp]$ be an interval for computation of the series solution of system (25). We cannot calculate the compartments $\mathcal{S}(t)$, $I(t)$, $I(t)$, $D(t)$ solution of the initial value problem (25). Instead of this, a set of points $(t_q, S(t_q))$ can be taken and their points are taken for our numerical scheme. Thus, we further subdivide the interval $[0, \wp]$ into i small subintervals $[t_q, t_{q+1}]$ of the same length $h = \wp/n$ only applying the nodes $t_q = qh$, for $q = 0, 1, \ldots, n$. Consider that

$$\mathcal{S}(t), I(t), R(t), D(t) {}^C\mathrm{D}_t^{\wp}\mathcal{S}(t), {}^C\mathrm{D}_t^{\wp}I(t), {}^C\mathrm{D}_t^{\wp}R(t), {}^C\mathrm{D}_t^{\wp}D(t)$$

and

$${}^C\mathrm{D}_t^{2\wp}\mathcal{S}(t), {}^C\mathrm{D}_t^{2\wp}I(t), {}^C\mathrm{D}_t^{2\wp}R(t), {}^C\mathrm{D}_t^{2\wp}D(t),$$

are continuous on $[0, T]$. Using the general Euler's or Taylor's method about $t = t_0 = 0$ to the considered problem given in Eq. (25) and for all t taking $a \in (0, T)$, the mathematical form for t_1, we have

$$\begin{aligned}
\mathcal{S}(t_1) &= \mathcal{S}(t_0) + \mho_1(t_0, \mathcal{S}(t_0), I(t_0), R(t_0), D(t_0))\frac{t^{\wp}}{\Gamma(\wp+1)} + {}^C\mathrm{D}_t^{2\wp}\mathcal{S}(t)|_{t=a}\frac{t^{2\wp}}{\Gamma(2\wp+1)},\\
I(t_1) &= I(t_0) + \mho_2(t_0, \mathcal{S}(t_0), I(t_0), R(t_0), D(t_0))\frac{t^{\wp}}{\Gamma(\wp+1)} + {}^C\mathrm{D}_t^{2\wp}I(t)|_{t=a}\frac{t^{2\wp}}{\Gamma(2\wp+1)},\\
R(t_1) &= R(t_0) + \mho_3(t_0, \mathcal{S}(t_0), I(t_0), R(t_0), D(t_0))\frac{t^{\wp}}{\Gamma(\wp+1)} + {}^C\mathrm{D}_t^{2\wp}R(t)|_{t=a}\frac{t^{2\wp}}{\Gamma(2\wp+1)},\\
D(t_1) &= D(t_0) + \mho_4(t_0, \mathcal{S}(t_0), I(t_0), R(t_0), D(t_0))\frac{t^{\wp}}{\Gamma(\wp+1)} + {}^C\mathrm{D}_t^{2\wp}D(t)|_{t=a}\frac{t^{2\wp}}{\Gamma(2\wp+1)}.
\end{aligned} \tag{26}$$

Taking the value of h very small then we omit the heist power of h, then we may remove the high-order terms having $h^{2\theta}$ and get Eq. (26) as

$$\begin{aligned}
\mathcal{S}(t_1) &= \mathcal{S}(t_0) + \mho_1(t_0, \mathcal{S}(t_0), I(t_0), R(t_0), D(t_0))\frac{t^{\wp}}{\Gamma(\wp+1)},\\
I(t_1) &= I(t_0) + \mho_2(t_0, \mathcal{S}(t_0), I(t_0), R(t_0), D(t_0))\frac{t^{\wp}}{\Gamma(\wp+1)},\\
R(t_1) &= R(t_0) + \mho_3(t_0, \mathcal{S}(t_0), I(t_0), R(t_0), D(t_0))\frac{t^{\wp}}{\Gamma(\wp+1)},\\
D(t_1) &= D(t_0) + \mho_4(t_0, \mathcal{S}(t_0), I(t_0), R(t_0), D(t_0))\frac{t^{\wp}}{\Gamma(\wp+1)}.
\end{aligned} \tag{27}$$

On writing again by the same method, a set of points that approximated the solution $(\mathcal{S}(t), I(t), R(t), D(t))$ is obtained. The generalized formula on $t_{q+1} = t_q + h$ is

$$\begin{aligned}
\mathcal{S}(t_{q+1}) &= \mathcal{S}(t_q) + \mho_1(t_q, \mathcal{S}(t_q), I(t_q), R(t_q), D(t_q))\frac{h^{\wp}}{\Gamma(\wp+1)},\\
I(t_{q+1}) &= I(t_q) + \mho_2(t_q, \mathcal{S}(t_q), I(t_q), R(t_q), D(t_q))\frac{h^{\wp}}{\Gamma(\wp+1)},\\
R(t_{q+1}) &= R(t_q) + \mho_3(t_q, \mathcal{S}(t_q), I(t_q), R(t_q), D(t_q))\frac{h^{\wp}}{\Gamma(\wp+1)},\\
D(t_{q+1}) &= D(t_q) + \mho_4(t_q, \mathcal{S}(t_q), I(t_q), R(t_q), D(t_q))\frac{h^{\wp}}{\Gamma(\wp+1)},
\end{aligned} \tag{28}$$

where $q = 0, 1, 2, \ldots, n-1$.

7 Computational of the numerical solution of the COVID-19 model for model (2)

In this section, we investigate the numerical solution of the COVID-19 model (2). For this we need to take the following values for the concerned parameter of the model, and we consider the initial values as: $r = 0.0000033$, $a = 0.0000035$, $d = 0.019$, $\mathcal{S}_0 = 8.8$ million, $I_0 = 0.57$ million, $R_0 = 0.53$ million, and $D_0 = 0.015$ million as,

$$\begin{cases} \mathcal{S}'(t_0) = -0.00001655, \\ \mathcal{S}''(t_0) = 0.000000314, \\ \mathcal{S}'''(t_0) = -0.00000000631, \\ \mathcal{S}^{iv}(t_0) = 0.000000000923, \\ \mathcal{S}^{v}(t_0) = -0.000000002123. \end{cases} \tag{29}$$

$$\begin{cases} I'(t_0) = -0.01081544, \\ I''(t_0) = 0.0002022, \\ I'''(t_0) = -0.00000356, \\ I^{iv}(t_0) = 0.0000000471, \\ I^{v}(t_0) = -0.00000000635. \end{cases} \tag{30}$$

$$\begin{cases} R'(t_0) = 0.00000199, \\ R''(t_0) = -0.000000664, \\ R'''(t_0) = 0.000000000717, \\ R^{iv}(t_0) = -0.00003522, \\ R^{v}(t_0) = 0.00000357. \end{cases} \tag{31}$$

$$\begin{cases} D'(t_0) = 0.01083, \\ D''(t_0) = -0.000205, \\ D'''(t_0) = 0.00000389, \\ D^{iv}(t_0) = -0.0000000739, \\ D^{v}(t_0) = 0.000000001125. \end{cases} \tag{32}$$

Plugging the values of Eqs. (29)–(32) in Eq. (21), we obtain

$$\begin{cases} \mathcal{S}(t) = 8.8 + t(-0.00001655) + \dfrac{t^2}{2!}(0.000000314) + \dfrac{t^3}{3!}(-0.00000000631) \\ \qquad + \dfrac{t^4}{4!}(0.000000000923) + \dfrac{t^5}{5!}(-0.0000000002123) + \cdots, \\ I(t) = 0.57 + t(-0.01081544) + \dfrac{t^2}{2!}(0.0002022) + \dfrac{t^3}{3!}(-0.00000356) \\ \qquad + \dfrac{t4}{4!}(0.0000000471) + \dfrac{t^5}{5!}(-0.00000000635) + \cdots, \\ R(t) = 0.53 + t(0.00000199) + \dfrac{t^2}{2!}(-0.000000664) + \dfrac{t^3}{3!}(0.000000000717) \\ \qquad + \dfrac{t^4}{4!}(-0.00003522) + \dfrac{t^5}{5!}(0.00000357) + \cdots, \\ D(t) = 0.015 + t(0.01083) + \dfrac{t^2}{2!}(-0.000205) + \dfrac{t^3}{3!}(0.00000389) \\ \qquad + \dfrac{t^4}{4!}(-0.0000000739) + \dfrac{t^5}{5!}(0.000000001125) + \cdots. \end{cases} \tag{33}$$

The series solution uses the following values of the parameters: $r = 0.0000033$, $a = 0.0000035$, $d = 0.019$, $\mathcal{S}_0 = 8.8$ million, $I_0 = 0.57$ million, $R_0 = 0.53$ million, and $D_0 = 0.015$ million. We can write

$$\begin{cases} \mathcal{S}(t) = \displaystyle\sum_{k=0}^{\infty} \frac{\mathcal{S}^k(t_0)}{k!} t^k, \quad I(t) = \sum_{k=0}^{\infty} \frac{I^k(t_0)}{k!} t^k, \\ R(t) = \displaystyle\sum_{k=0}^{\infty} \frac{R^k(t_0)}{k!} t^k, \quad D(t) = \sum_{k=0}^{\infty} \frac{D^k(t_0)}{k!} t^k. \end{cases} \tag{34}$$

By using software like Mathematica, we plot the solution up to 100 terms as shown in Figs. 1–4. From the plot given in Figs. 1–4 we see that the Taylor's series is a powerful technique for finding the numerical solution of the nonlinear problem.

In Figs. 1–4, we have provided graphical representations of different classes for the proposed model.

8 Graphical results and discussion for model (3)

To present the concerned approximate solutions (28) of the model under consideration, we recall some numerical values for the parameters in Table 1. Figs. 5–8 are the representations of all the four compartments of the model (3) at various fractional orders by Euler's method using data I, similar to the data used for the integer-order problem (2). Both the approaches of the integer-order model and the fraction-order model are comparable with each other and by increasing the fractional values will converge to the integer values. Also in data I we can see that $r < a + d$; this means that the infection will vanish, as can be seen from Fig. 6.

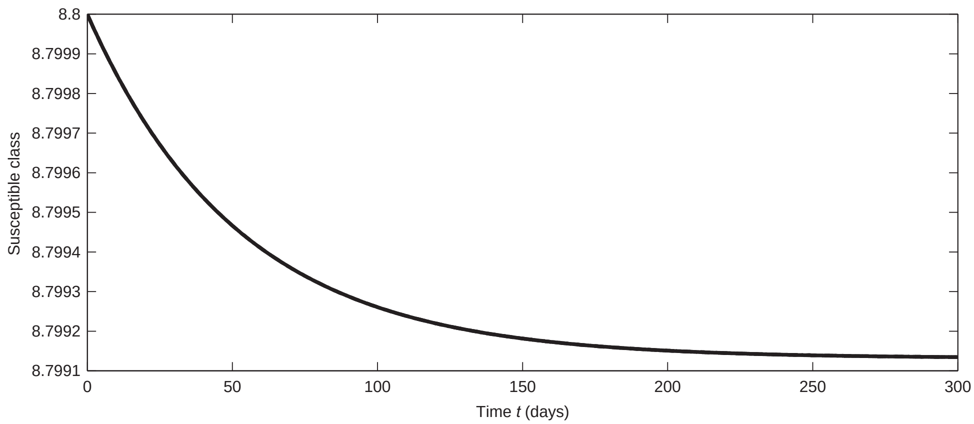

FIG. 1 Dynamical behavior of susceptible class.

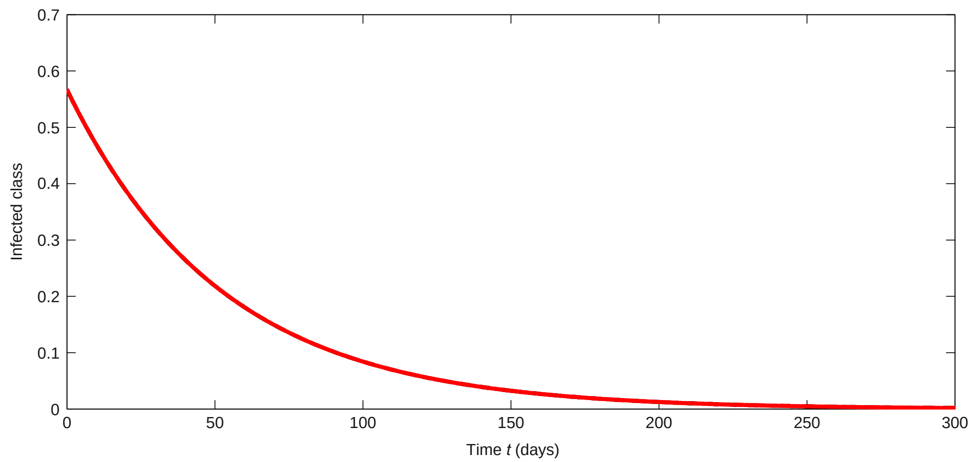

FIG. 2 Dynamical behavior of infected class.

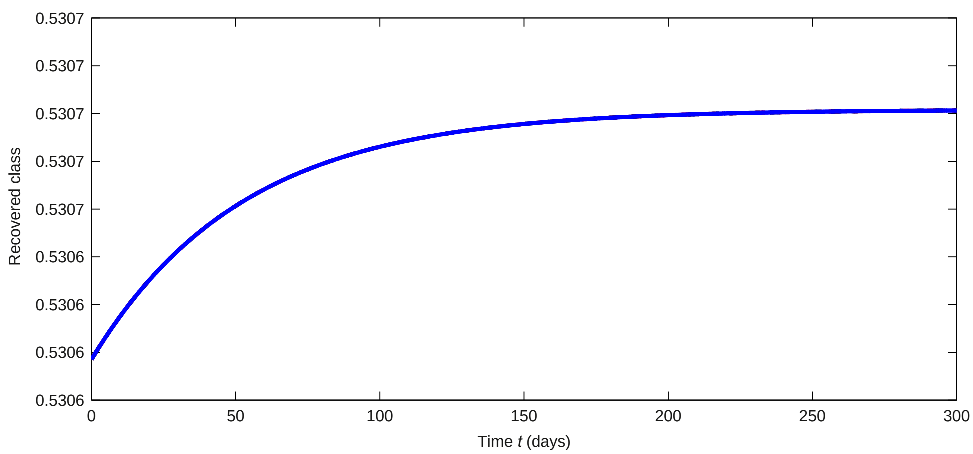

FIG. 3 Dynamical behavior of recovered class.

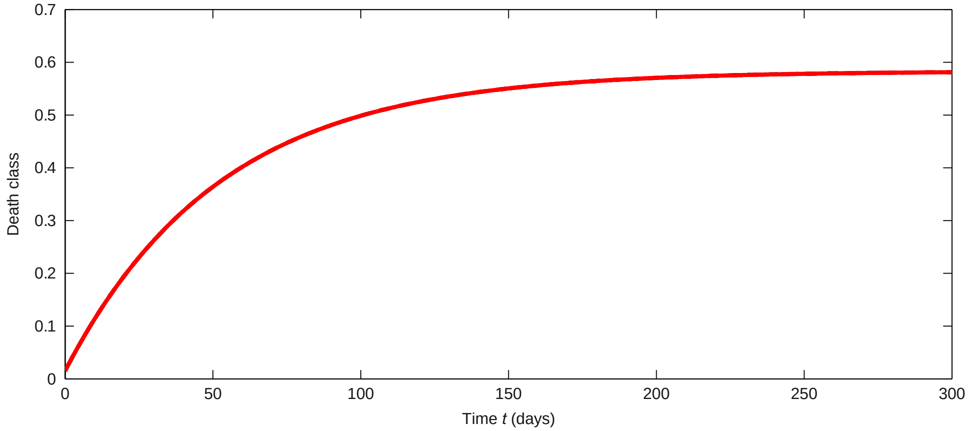

FIG. 4 Dynamical behavior of death class.

Table 1 Parametric values for our model (3).

Parameters	Data I	Data II	Data III
S_0	8.8 million	8.8 million	8.8 million
I_0	0.57 million	0.57 million	0.57 million
R_0	0.53 million	0.53 million	0.53 million
D_0	0.015 million	0.015 million	0.015 million
a	0.0000035	0.00000030	0.00003
d	0.019	0.00000033	0.000003
r	0.0000036	0.00000003	0.00058

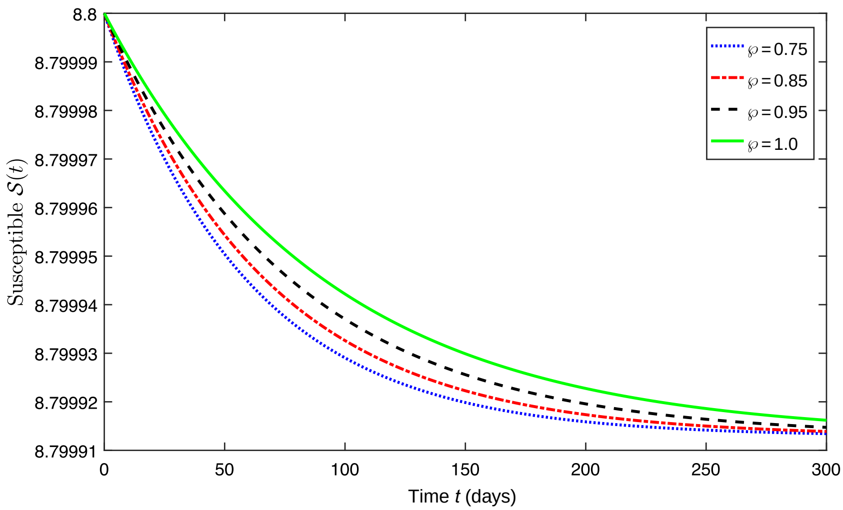

FIG. 5 Graphical representation of numerical solution for $S(t)$ at various arbitrary order of $\wp$ for data I.

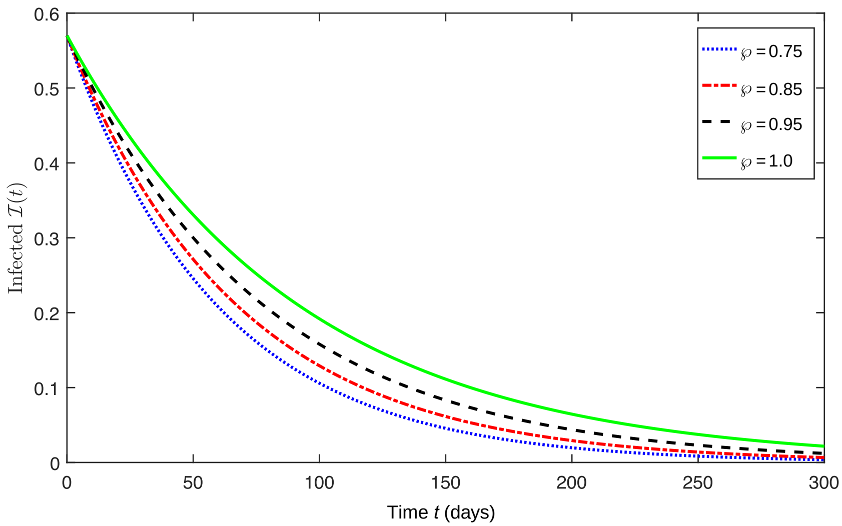

FIG. 6 Graphical representation of numerical solution for $I(t)$ at various arbitrary order of $\wp$ for data I.

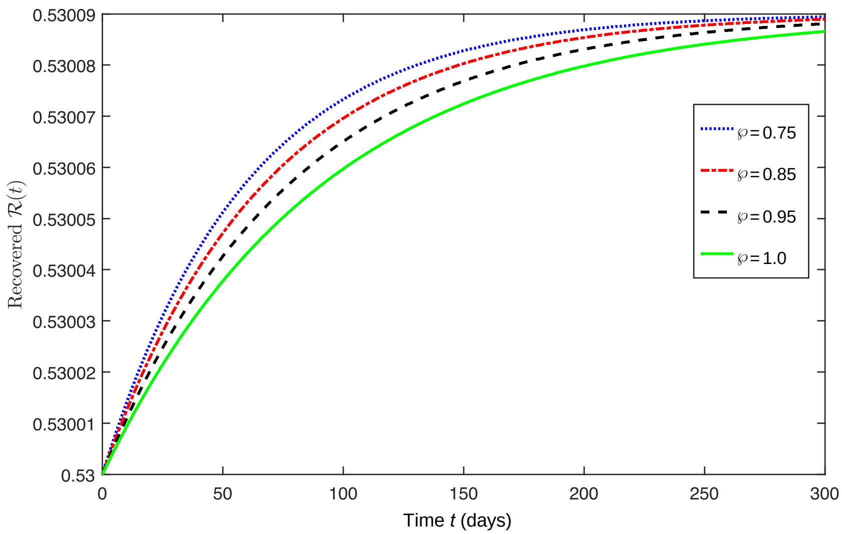

FIG. 7 Graphical representation of numerical solution for $R(t)$ at various arbitrary order of $\wp$ for data I.

Figs. 9–12 are representations of different compartments of model (3) at different fractional orders for data II. In this case $r = a + d$, which implies that if $\mathcal{S}(t) = 1$ then no pandemic will occur, as can be seen from Fig. 10, or there will be very small amounts of infection.

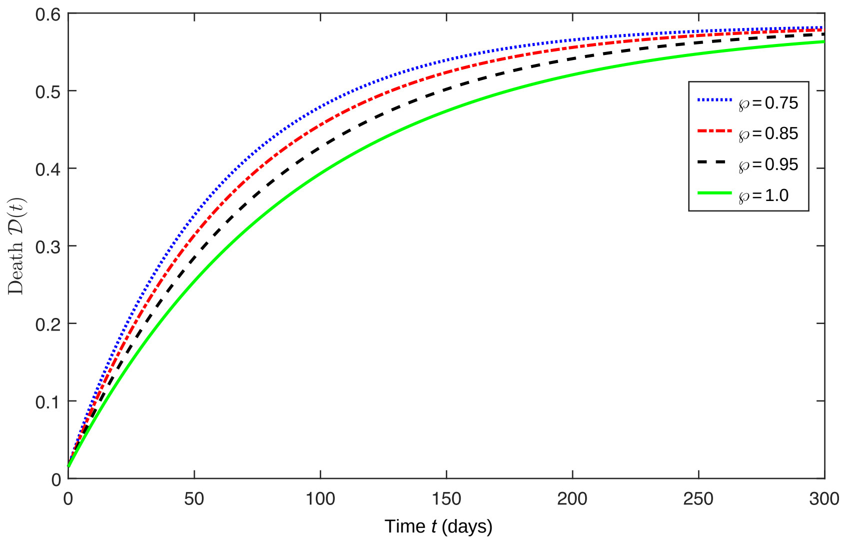

FIG. 8 Graphical representation of numerical solution for $D(t)$ at various arbitrary order of $\wp$ for data I.

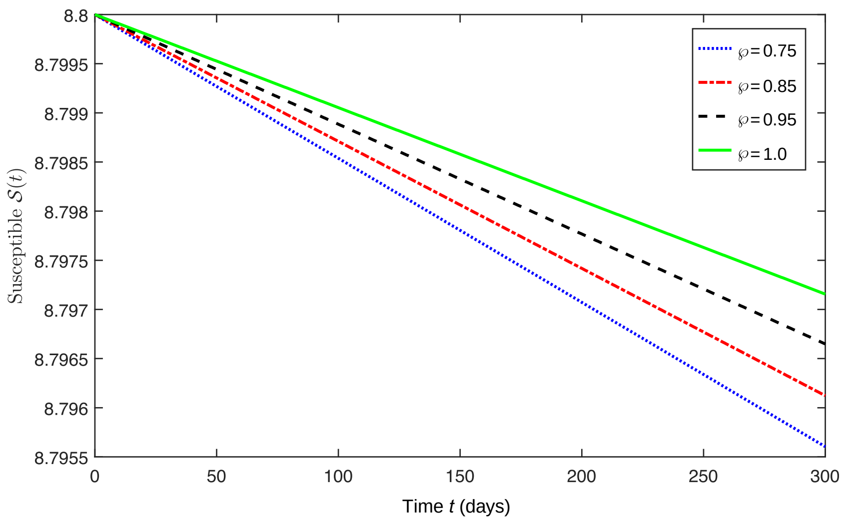

FIG. 9 Graphical representation of numerical solution for $S(t)$ at various arbitrary order of $\wp$ for data II.

Figs. 13–16 are the representation of all agent of model (3) for data III at different fractional orders of $\wp$. Here $r > a + d$, which means that the infection will occur and will be increasing as can be seen from Fig. 14.

9 Concluding remarks

In this chapter, we have studied a four-compartmental mathematical model of COVID-19 in both integer and fractional orders. The concerned model consist of susceptible,

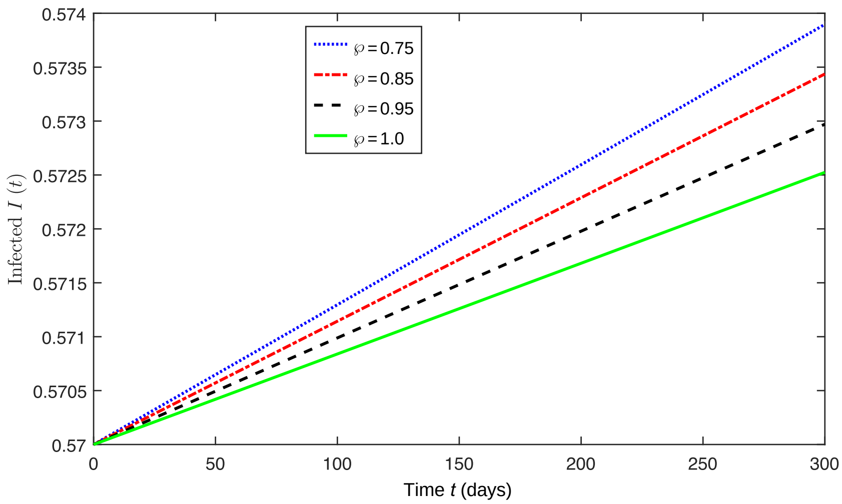

FIG. 10 Graphical representation of numerical solution for $S(t)$ at various arbitrary order of $\wp$ for data II.

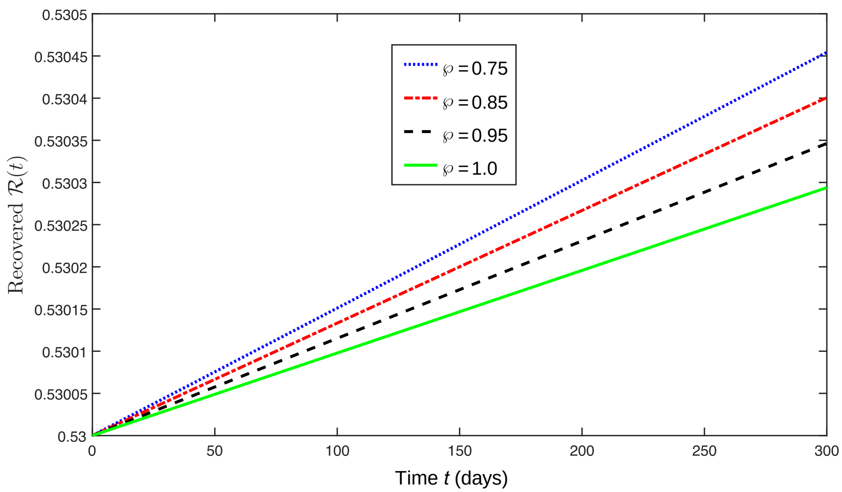

FIG. 11 Graphical representation of numerical solution for $S(t)$ at various arbitrary order of $\wp$ for data II.

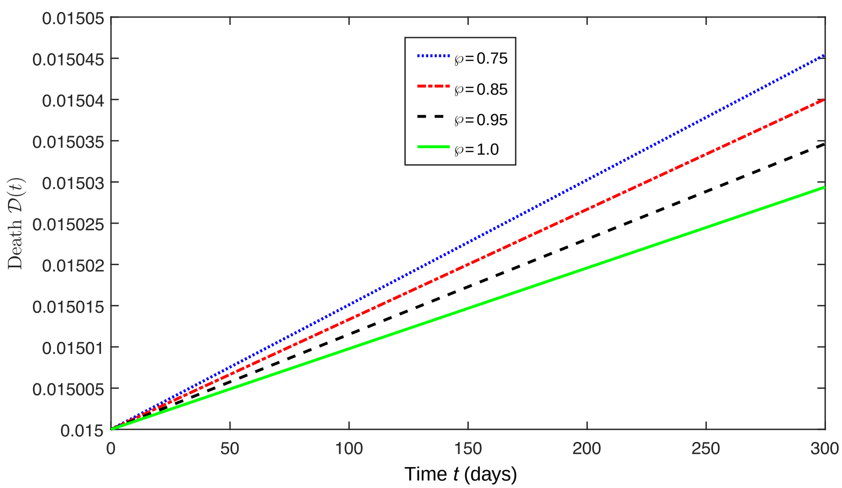

FIG. 12 Graphical representation of numerical solution for $S(t)$ at various arbitrary order of $\wp$ for data II.

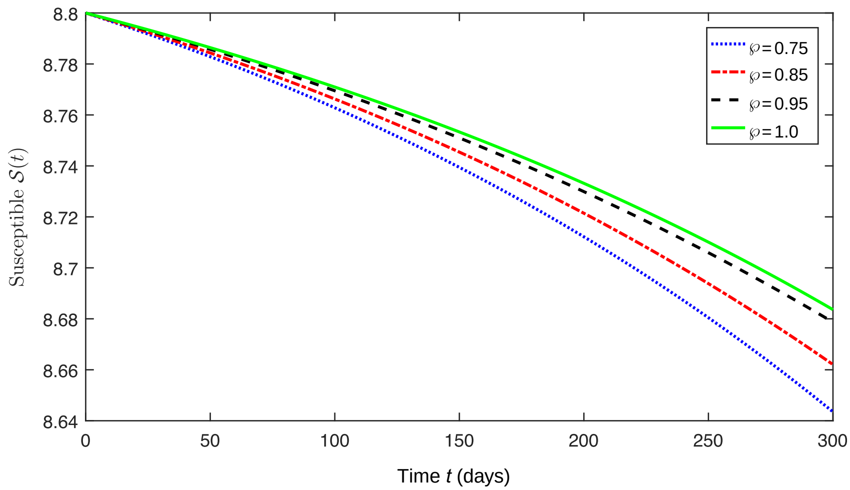

FIG. 13 Graphical representation of numerical solution for $S(t)$ at various arbitrary order of $\wp$ for data III.

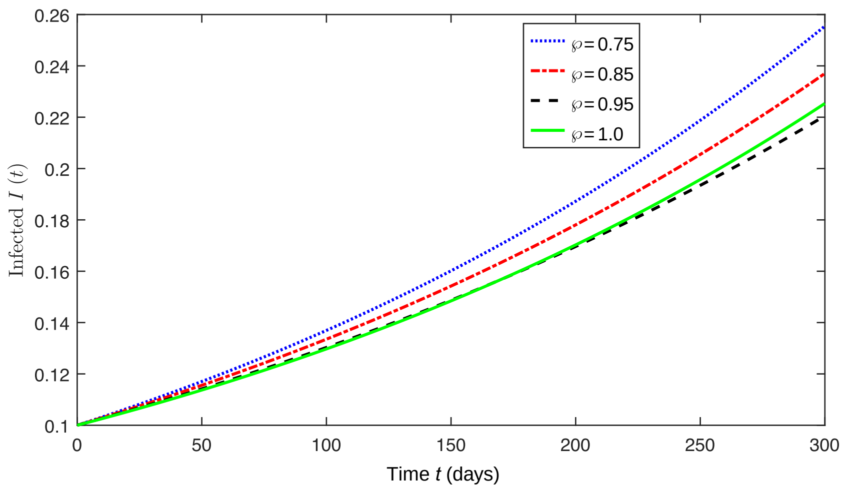

FIG. 14 Graphical representation of numerical solution for $S(t)$ at various arbitrary order of $\wp$ for data III.

infected, recovered, and death classes. The feasibility and stability analysis of the proposed fractional-order model has been achieved by the techniques of basic reproduction number. The fractional-order model has also been analyzed for existence and uniqueness of solution using some well-known theorems of fixed-point theory. We have investigated the general and numerical solution for the proposed COVID-19 model through the Taylor's series method to compute a series solution to the considered models of integer and

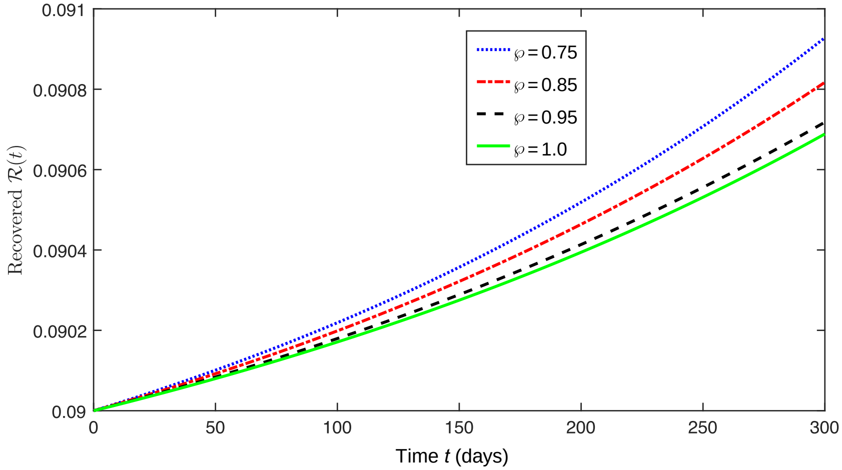

FIG. 15 Graphical representation of numerical solution for $S(t)$ at various arbitrary order of $\wp$ for data III.

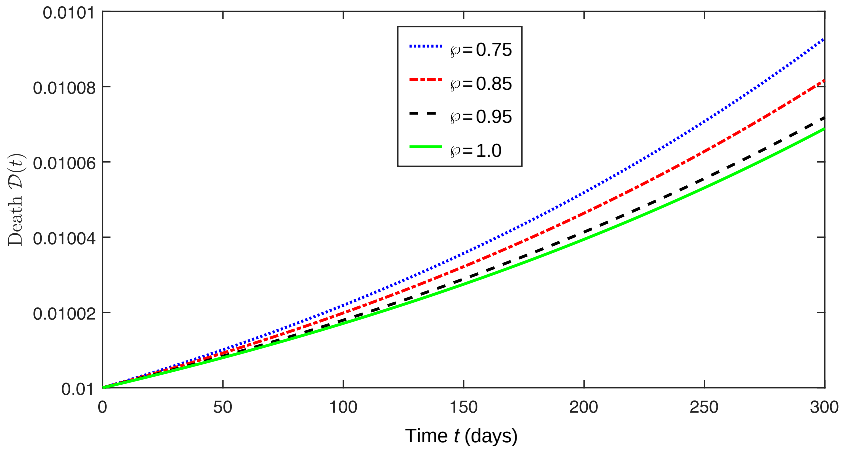

FIG. 16 Graphical representation of numerical solution for $S(t)$ at various arbitrary order of $\wp$ for data III.

fractional order, for three different values of parameter in the considered model. The propose schemes have been simulated to show the validity of our proposed schemes and the investigation of fractional-order calculus. Both the numerical schemes are comparable with each other. The proposed techniques of qualitative, stability, and numerical analysis may be applied to various integer and fractional-order differential equations or mathematical models representing some real-world phenomena.

References

[1] World Health Organization, Coronavirus disease 2019 (COVID-19) Situation Report-62, https://www.who.int/docs/default-source/coronaviruse/situation-reports/20200322-sitrep-62-covid-19.pdf?sfvrsn=f7764c462, 2020.

[2] Ensheng D, Hongru D, Lauren G. An interactive web-based dashboard to track COVID-19 in real time. Lancet Infect Dis 2020;20(5):533–4.

[3] Sha H, Sanyi T, Libin R. A discrete stochastic model of the COVID-19 outbreak. Forecast Control Math Biosci Eng 2020;17(4):2792–804.

[4] Gao W, Veeresha P, Prakasha DG, Baskonus HM, Yel G. New approach for the model describing the deathly disease in pregnant women using Mittag-Leffler function. Chaos Solit Fractals 2020;134:109696.

[5] Andrew T, Smith P. The Health of Nations: Infectious Disease, Environmental Change and Their Effects on National Security and Development. Cambridge: MIT Press; 2001.

[6] Salath M, Althaus CL, Neher R, Stringhini S, Hodcroft E, Fellay J, Zwahlen M, Senti G, Battegay M, Smith AW. COVID-19 epidemic in Switzerland: on the importance of testing, contact tracing and isolation. Swiss Med Wkly 2020;150:1112.

[7] Fisher D, Heymann D. The novel coronavirus outbreak causing COVID-19. BMC Med 2020;18(1):1–3.

[8] Xiaohua Y, Chang L, Hanjie W, Henning FJ. The impact of COVID-19 on food prices in China: evidence of four major food products from Beijing, Shandong and Hubei Provinces. China Agric Econ Rev 2020;12(3):445–58.

[9] Yousaf M, Zahir S, Riaz M, Hussain SM, Shah K. Statistical analysis of forecasting COVID-19 for upcoming month in Pakistan. Chaos Solit Fractals 2020;138:109926.

[10] Ren X. Pandemic and lockdown: a territorial approach to COVID-19 in China, Italy and the United States. Eurasian Geogr Econ 2020;61(4–5):423–34.

[11] Guidotti E, Ardia D. COVID-19 Data Hub. J Open Source Software 2020;5(51):2376.

[12] Hurwitz JL. B cells, viruses and the SARS-CoV-2/COVID-19 pandemic of 2020. Viral Immunol 2020;33(4):251–2.

[13] Goyal M, Baskonus HM, Prakash A. An efficient technique for a time fractional model of Lassa hemorrhagic fever spreading in pregnant women. Eur Phys J Plus 2019;134(481):1–10.

[14] Gao W, Veeresha P, Prakasha DG, Baskonus HM, Yel G. New approach for the model describing the deathly disease in pregnant women using Mittag-Leffler function. Chaos Solit Fractals 2020;134:109696.

[15] Kumar D, Singh J, Al-Qurashi M, Baleanu D. A new fractional SIRS-SI malaria disease model with application of vaccines, anti-malarial drugs, and spraying. Adv Differ Equ 2019;278:1–10.

[16] Shah K, Alqudah MA, Jarad F, Abdeljawad T. Semi-analytical study of Pine Wilt disease model with convex rate under Caputo-Febrizio fractional order derivative. Chaos Solit Fractals 2020;135:109754.

[17] Tian X, et al. Potent binding of 2019 novel coronavirus spike protein by a SARS coronavirus-specific human monoclonal antibody. Emer Micr Inf 2020;9(1):382–5.

[18] Ge XY, et al. Isolation and characterization of a bat SARS-like coronavirus that uses the ACE2 receptor. Nature 2013;503:535–8.

[19] Jasper FWC, et al. Genomic characterization of the 2019 novel human-pathogenic coronavirus isolated from patients with acute respiratory disease in Wuhan Hubei, China. Emerg Microbes Infect 2020;9(1):221–36.

[20] Lu H, et al. Outbreak of pneumonia of unknown etiology in Wuhan China: the mystery and the miracle. J Med Virol 2020;92(4):401.

[21] Riou J, Althaus CL. Pattern of early human-to-human transmission of Wuhan 2019 novel coronavirus (2019-nCoV), December 2019 to January 2020. Euro Surveill 2020;25(4):2000058.

[22] Lin Q, et al. A conceptual model for the coronavirus disease 2019 (COVID-19) outbreak in Wuhan, China with individual reaction and governmental action. Int J Inf Dis 2020;93:211–6.

[23] Bonyah E, Ogunlade S, Purohit SD, Singh J. Modelling culture hereditary transmission: insight through optimal control. Ecol Complex 2021;45:100890.

[24] Habenom H, Suthar DL, Baleanu D, Purohit SD. A numerical simulation on the effect of vaccination and treatments for the fractional hepatitis B model. ASME J Comput Nonlinear Dyn 2021;16 (1):011004.

[25] Singh H, Singh J, Purohit SD, Kumar D. Advanced Numerical Methods for Differential Equations: Applications in Science and Engineering. New York: CRC Press; Taylor & Francis; 2021.

[26] Singh H, Kumar D, Baleanu D. Methods of Mathematical Modelling: Fractional Differential Equations. New York: CRC Press; Taylor & Francis; 2019.

[27] Lakshmikantham V, Leela S. Naguma-type uniqueness result for fractional differential Equations. Nonlinear Anal 2009;71:2886–9.

[28] Lotka JA. Contribution to the theory of periodic reactions. J Phys Chem 2002;14(3):271–4.

[29] Podlubny I. Fractional Differential Equations. New York: Academic Press; 1999.

[30] Lakshmikantham V, Leela S, Vasundhara J. Theory of Fractional Dynamic Systems. Cambridge: Cambridge Academic Publishers; 2009.

[31] Singh H. Analysis for fractional dynamics of Ebola virus model. Chaos Solit Fractals 2020;138:109992.

[32] Singh H. Analysis of drug treatment of the fractional HIV infection model of $CD4^+$ T-cells. Chaos Solit Fractals 2020;146:110868.

[33] Singh H, Srivastava HM, Hammouch Z, Nisar KS. Numerical simulation and stability analysis for the fractional-order dynamics of COVID-19. Results Phys 2021;20:103722.

[34] Singh H, Baleanu D, Singh J, Dutta H. Computational study of fractional order smoking model. Chaos Solit Fractals 2020;142:110440.

[35] Singh H. Jacobi collocation method for the fractional advection-dispersion equation arising in porous media. Numer Methods Partial Differ Equ 2020;1–18. https://doi.org/10.1002/num.22674.

[36] Singh H. Numerical simulation for fractional delay differential equations. Int J Dyn Control 2021;9 (2):463–74.

[37] Singh H, Singh AK. Numerical simulation for fractional Bloch equation arising in nuclear magnetic resonance. Nonlinear Stud 2021;28:531–48.

[38] Hilfer R. Applications of Fractional Calculus in Physics. Singapore: World Scientific; 2000.

[39] Rahman NAA, Ahmad MZ. Solving fuzzy fractional differential equations using fuzzy Sumudu transform. J Nonlinear Sci Appl 2017;10:2620–32.

[40] Rossikhin YA, Shitikova MV. Applications of fractional calculus to dynamic problems of linear and nonlinear hereditary mechanics of solids. Appl Mech Rev 1997;50:15–67.

[41] Baleanu D, Mousalou A, Rezapour S. A new method for investigating approximate solutions of some fractional integro-differential equations involving the Caputo-Fabrizio derivative. Adv Differ Equ 2017;2017:51.